Analogue experiments on releasing and restraining bends and their application to the study of the Barents Shear Margin

Roy H. Gabrielsen[1], Panagiotis A. Giennenas[2], Dimitrios Sokoutis[1,3], Ernst Willingshofer[3], Muhammad Hassaan[1,4] & Jan Inge Faleide[1]

[1]Department of Geosciences, University of Oslo, Norway
[2]panagiotis-athanasios.giannenos@univ-rennes1.fr
[3]Faculty of Geosciences, Utrecht University, the Netherlands
[4]Vår Energi AS, Grundingen 3, 0250 Oslo, Norway

Corresponding author: Roy H. Gabrielsen (r.h.gabrielsen@geo.uio.no)

ORCI-id:
Jan Inge Faleide: 0000-0001-8032-2015
Roy H. Gabrielsen: 0000-0001-5427-8404
Muhammad Hassaan: 0000-0001-6004-8557

Abstract:
The Barents Shear Margin separates the Svalbard and Barents Sea from the North Atlantic. During the break-up of the North Atlantic the plate tectonic configuration was characterized by sequential dextral shear, extension, and finally contraction and inversion. This generated a complex zone of deformation that contains several structural families of overlapping and reactivated structures. A series of crustal-scale analogue experiments, utilizing a scaled stratified sand-silicon polymer sequence were utilized in the study of the structural evolution of the shear margin.

The most significant observations of particular significance for interpreting the structural configuration of the Barents Shear Margin are:
1) Prominent early-stage positive structural elements (e.g. folds, push-ups) interacted with younger (e.g. inversion) structures and contributed to a hybrid final structural pattern.
2) Several of the structural features that were initiated during the early (dextral shear) stage became overprinted and obliterated in the subsequent stages.
3) All master faults, pull-part basins and extensional shear duplexes initiated during the shear stage quickly became linked in the extension stage, generating a connected basin system along the entire shear margin at the stage of maximum extension.
4) The fold pattern generated during the terminal stage (contraction/inversion became dominant in the basin areas and was characterized by fold axes with traces striking parallel to the basin margins. These folds, however, most strongly affected the shallow intra-basin layers.
The experiments reproduced the geometry and positions of the major basins and relations between structural elements (fault and fold systems) as observed along

and adjacent to the Barents Shear Margin. This supports the present structural model for the shear margin.

Plain language summary:

The Barents Shear Margin defines the border between the relatively shallow Barents Sea that is situated on a continental plate, and the deep ocean. The margin is characterized by a complex structural pattern that has resulted from the opening and separation of the continent and the ocean, starting c. 55 million years ago. This history included one phase of right-lateral shear and one phase of oblique extension, the latter including a subphase of shortening, perhaps due to plate tectonic reorganizations. The area has been mapped by the study of reflection seismic lines for decades, but many details of its development is not yet fully constrained. We therefore ran a set of scaled experiments to investigate what kind of structures could be expected in this kind of tectonic environment, and to figure out what is a reasonable time relation between them. From these experiments we deducted several types of structures/faults, folds and sedimentary basins) that helps us to improve the understanding of the history of the opening of the North Atlantic.

Key words: Analogue experiments, dextral strike-slip, releasing and restraining bends, multiple folding, Barents Shear Margin**,** basin inversion

Introduction

Physiography, width and structural style of the Norwegian continental margin vary considerably along its strike (e.g. Faleide et al., 2008, 2015). The margin includes a southern rifted segment between 60^{o} and 70^{o}N and a northern sheared-rifted segment between 70^{o} and 82^{o}N (**Figure 1A**). The latter coincides with the ocean-ward border of the western Barents Sea and Svalbard margins (e.g. Faleide et al., 2008) and is referred to here as "the Barents Shear Margin". This segment coincides with the continent-ocean transition (COT) of the northernmost part of the North Atlantic Ocean, and its configuration is typical for that of transform margins where the structural pattern became established in an early stage of shear, later to develop into an active continent-ocean passive margin (Mascle & Blarez, 1987; Lorenzo, 1997; Seiler et al., 2010; Basile, 2015; Nemcok et al., 2016). Palaeogene shear, rifting, breakup and incipient spreading in the North Atlantic was associated with voluminous magmatic activity, resulting in the development of the North Atlantic Volcanic Province (Saunders et al., 1997; Ganerød et al., 2010; Horni et al., 2017). According to its tectonic development, the Barents Shear Margin (**Figure 1B**) incorporates, or is bordered by, several distinct structural elements, some of which are associated with volcanism and halokinesis.

The multistage development combined with a complex geometry caused interference between structures (and sediment systems) in different stages of the margin development. Such relations are not always obvious, but interpretation can be supported by the help of scaled experiments. In combining the interpretation of reflection seismic data and analogue modeling, therefore, we investigate structures generated in (initial) dextral shear, the development into seafloor spreading and subsequent contraction in this process, the later stages of which were likely influenced by plate reorganization (Talwani & Eldholm, 1977; Gaina et al., 2009; see also Vågnes et al., 1998; Pascal & Gabrielsen, 2001; Pascal et al., 2005; Gac et al., 2016) and/or other far-field stresses (Doré & Lundin, 1996; Lundin & Doré, 1997; Doré et al., 1999; 2016; Lundin et al., 2013). The present experiments were designed to illuminate the structural complexity affiliated with multistage sheared passive margins, so that the significance of structural elements like fault and fold systems observed along the Barents Shear Margin could be set

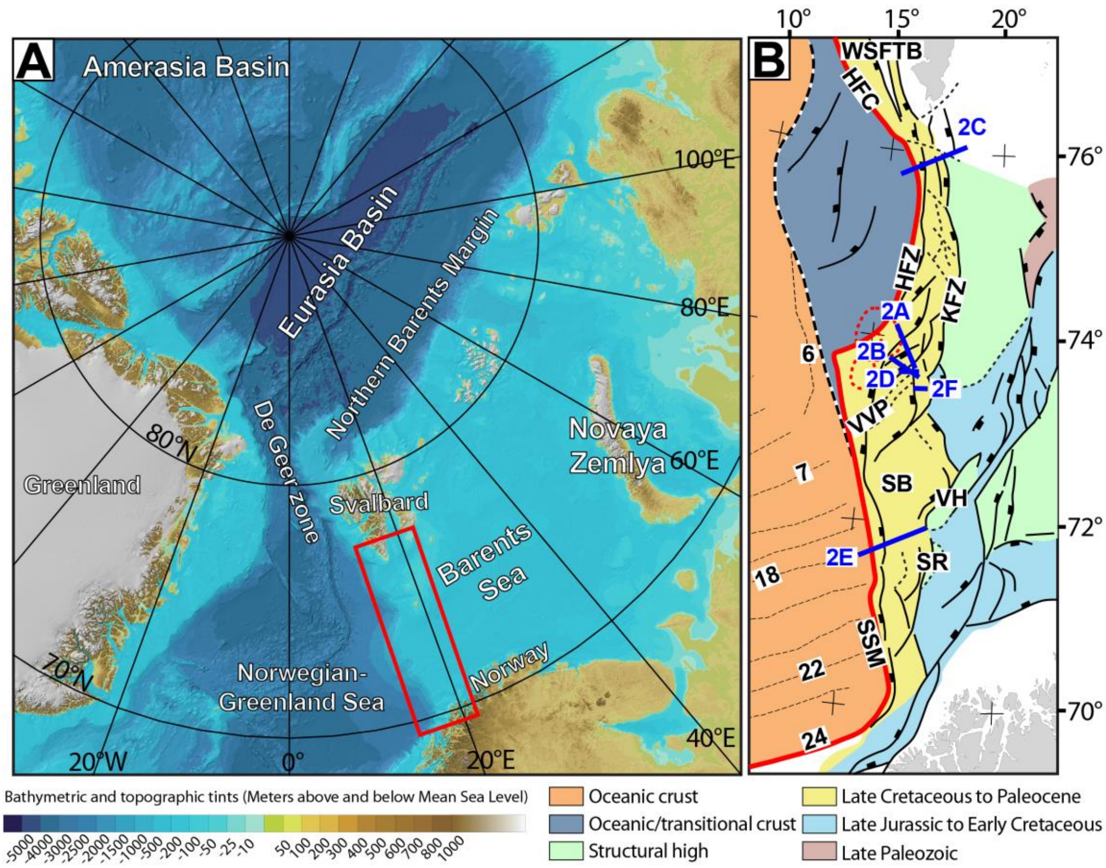

Figure 1: A) The Barents Sea provides is separated from the Norwegian-Greenland Sea by the De Geer Zone linking the North Atlantic to the Arctic Eurasia Basin. Red box shows the present study area. **B)** Structural map Barents Sea shear margin. Note segmentation of the continent-ocean transition. Abbreviations (from north to south): WSFTB = West Spitsbergen Fold-and-Thrust Belt, HFZ = Hornsund Fault Zone, KFZ = Knølegga Fault Zone, VVP = Vestbakken Volcanic Province, SB = Sørvestsnaget Basin, VH = Veslemøy High, SR = Senja Ridge, SSM = Senja Shear Margin. Blue lines indicate position of seismic profiles in Figure 2 and red line in Figure 1B shows the western limitation of the thinned crust (see also Figure 3). Chron numbers are indicated on oceanic crust area.

into a dynamic context. The study area suffered repeated and contrasting stages of deformation, including dextral shear, oblique extension, inversion and volcanic activity. This is a particular challenge in such tectonic settings, that are characterized by repeated overprinting and canabalization of incipient by younger structural elements. The experimental approach opens for the identification and characterisation of the different stages of deformation and their affiliated structural elements on the way to the present-day margin geometry.

Regional setting

In the following sections we provide definitions and a short description of the most important structural elements constituting the study area. The structural elemnts are presented in-sequence from north to south (**Figure 1B**).

The greater **Barents Shear Margin** is a part of the preceeding and more extensive "De Geer Zone megashear system which linked the Norwegian Greenland Sea and the Arctic Eurasia Basin system (Eldholm et al., 1987; 2002; Faleide et al., 1988; Breivik et al., 1998; 2003). Together with its conjugate Greenland counterpart it carries the evidence of an extensive period of structural development, starting with post-Caledonian (Devonian) extension and culminating with Palaeogene break-up of the North Atlantic (e.g., Brekke, 2000; Gabrielsen et al., 1990; Faleide et al., 1993; 2008; Gudlaugsson et al., 1998; Tsikalas et al., 2012). Two shear margin segments that are separated by a central rift-dominated segment can be identified in the Barents Shear Margin (Myhre et al., 1982; Vågnes, 1997; Myhre & Eldholm, 1988; Ryseth et al., 2003; Faleide at al., 1988; 1993; 2008). Each segment maintained a particular signature concerning the structural and magmatic characteristics of the crust during its development. Of these the Senja Shear Margin is the southernmost segment, originally termed the Senja Fracture Zone by Eldholm et al. (1987). Here, NNW-SSE-striking folds interfere with folds with NE-SW-striking axes. Strain partitioning may also have affected some of the other shear zone segments of the study area (Sørvestsnaget Basin; Kristensen et al., 2017). Shearing contributed to the development of releasing and restraining bends, associated pull-apart-basins, neutral strike-slip segments, flower-structures and fold-systems (*sensu* Crowell, 1974 a,b; Biddle & Christie-Blick, 1985a,b; Cunningham & Mann, 2007a,b). Particularly the hanging wall west of the Knølegga Fault Complex (see below) of the Barents Shear Margin was affected by wrench deformation as seen from several push-ups and fold systems (Grogan et al., 1999; Bergh & Grogan 2003).

The Hornsund Fault Zone and West Spitsbergen Fold-and-Thrust Belt form the northernmost segment of the Barents Shear Margin and coincide with the northern continuation of the De Geer Zone. The presently distinguishable master fault of this system is the Hornsund Fault Zone, which together with the West Spitsbergen fold-and-thrust belt provides a type setting for transpression and strain partitioning (Harland, 1965; 1969; 1971; Lowell, 1972; Gabrielsen et al., 1992; Maher et al., 1997; Leever et al., 2011 a,b). Plate tectonic reconstructions suggest that the plate boundary accommodated c. 750 km along-strike displacement and 20-40 km of shortening in the Eocene (Bergh et al., 1997; Gaina et al., 2009).

The Knølegga Fault Zone can be seen as a part of the Hornsund fault system extending from the southern tip of Spitsbergen (Gabrielsen et al., 1990). It trends NNE-SSW to N-S and defines the western margin of the Stappen High. The vertical displacement approaches 6 km, being the cumulative effect of several phases of faulting throughout Late Paleozoic, Mesozoic and Cenozoic times. The Cenozoic displacement may have had a lateral (dextral) component (Gabrielsen et al., 1990).

The Vestbakken Volcanic Province is the central topic of the present contribution. It represents the rifted segment of the Barents Shear Margin and links the sheared margin segments that are situated to the north and south of it and occupies a typical right-double (eastward) stepping releasing-bend-setting. Prominent volcanoes and sill-intrusions display significant magmatic activity, and three distinct volcanic events are distinguished in the Vestbakken Volcanic Province (Jebsen & Faleide, 1998; Faleide et al., 2008; Libak et al., 2012). The area has been affected by complex tectonics and both extensional and contractional structures are observed. The Vestbakken Volcanic Province is delineated towards the east by an extensional top-west fault zone that parallels the Knølegga Fault Complex). The interior of the Vestbakken Volcanic Province is dominated by NE-SW-striking extensional faults and associated fault blocks. Positive structural elements include inverted fault blocks, and wide-angle (λ > 20 km) anticlines (roll-over anticlines?) and domes that are overprinted by faults and folds with amplitudes and wavelengths on the hundred- and km-scales.

The Eastern Boundary Fault (EBF) is a top-west normal fault with a regional NNE-SSW strike, consisting of two separate, linked segments. Its northern segment dips more steeply to the WNW than the southern segment. The total vertical displacement as measured on the early Eocene level is in the order of 300 ms (450 m), and the upper part of the hanging wall displays a normal drag modified by hanging wall tight anticline suggesting post-early Miocene inversion. Several normal, dominantly NE-SW-striking NW-facing normal faults transect the hanging wall of the EBF-fault. The Central Fault (CF) is the most prominent of those and is hard-linked to the central segment of the EBF-fault. All other faults in this map are secondary faults, mainly acting as accommodation structures to the master faults. Starting from the southern part of the area and south of the well site, a population of secondary faults is expressed as anastomosing faults traces.

Two main episodes of Cenozoic extensional faulting were identified in the Vestbakken Volcanic Province: (i) a late Paleocene-early Eocene event, which correlates in time with continental break-up in the Norwegian-Greenland Sea, and (ii) an early Oligocene event is tentatively correlated to plate reorganization around 34 Ma activating mainly NE-SW striking faults. Evidence of volcanic activity coincide with both of these events. Additional extensional events are recorded in mid-Eocene, late Oligocene and early Miocene times (Jebsen, 1998). The Vestbakken Volcanic Province is constrained to its east by the eastern boundary fault (EBF in **Figure 1B**), that is a part of the Knølegga Fault Zone, separating the Vestbakken Volcanic Province from the marginal Stappen High further to the east (Blaich et al., 2017). To the south and southeast the Vestbakken Volcanic Province drops gradually into the Sørvestsnaget Basin across the southern extension of the eastern boundary fault and its associated faults. To the west and north the area is delineated by the continent–ocean boundary/transition.

The Sørvestsnaget Basin occupies the area east of the COT between 71 and 73^{o}N and is characterized by an exceptionally thick Cretaceous-Cenozoic sequence (Gabrielsen et al., 1990). To the west it is delineated by the Senja Shear Margin and to the northeast it is separated from the Bjørnøya Basin by the southern part of the Knølegga Fault Complex (Faleide et al., 1988). The position of the Senja Ridge coincides with southeastern border of the Sørvestsnaget Basin (Figure 1B), whereas the Vestbakken Volcanic Province is situated to its north. An episode of Cretaceous rifting in the Sørvestsnaget Basin seems to have climaxed in the Cenomanian-middle Turonian (Breivik et al., 1998) to become succeeded by Late Cretaceous-Palaeocene fast sedimentation (Ryseth et al., 2003). Particularly the later stages of the basin development were strongly influenced by the opening of the North Atlantic (Hanisch, 1984; Brekke & Riis, 1987). Salt diapirism did also contribute to structuring of this basin (Perez-Garcia et al., 2013).

The Senja Ridge runs parallel to the continental margin and coincides with the western border of the Tromsø Basin. It is characterized by a N-S-trending gravity anomaly which are interpreted as buried mafic-ultramafic intrusions which are associated with the Seiland Igneous Province (Fichler & Pastore, 2022). The structural development of the Senja Ridge has been associated with shear affiliated with the development of the shear margin (Riis et al., 1986).

The Senja Shear Margin was active during the Eocene opening of the Norwegian-Greenland Sea during dextral shear that was accompanied by splitting out slivers of continental crust that became isolated units embedded by oceanic crust during seafloor spreading (Faleide et al., 2008). The Senja Shear Margin coincides with the western margin of a basin system that is characterized by significant crustal thinning and sedimentary thicknesses of 18-20 km. This part of the shear margin was characterized by a composite architecture even at the earliest stages of its development (Faleide et al., 2008). The structural development of the Senja Shear Margin was complicated by active halokinesis in the Sørvestsnaget Basin (Knutsen & Larsen, 1997; Gudlaugsson et al., 1998; Ryseth et al., 2003).

Data and structural interpretation

The data set of this study includes 2D seismic reflection data from several surveys and well data in the Vestbakken Volcanic Province. Data coverage is less dense in northern part of the study area. Typical spacing of seismic lines is 4 km. Well

7316/5-1 was used to correlate the seismic data with formation tops in the study area whereas published paper based correlations provided calibration and age of each seismic horizon mapped (e.g. Eidvin et al., 1993; 1998; Ryseth et al., 2003). Three stratigraphic groups are present in the well; the Nordland Group (473 - 945 m); the Sotbakken Group (945-3752m) and Nygrunnen Group (3752-4014m) (Eidvin et al., 1993; 1998; www.npd.com).

Several folds of regional significance and with axial traces that can be followed along strike for 2-3 km or more occur in the Vestbakken Volcanic Province. The folds commonly are situated in the hanging walls of extensional faults and the fold traces and the structural grain of the thick-skinned master faults are generally parallel. This shows that the position and orientation of the folds were determined by the preexisting structural fabric affiliated with these faults. The continuity of the folds remains obscure due to spacing of refection seismic lines, so each fold may include undetected overlap zones or axial off-sets that have not been detected. The folds were identified on the lower Eocene, Oligocene and lower Miocene levels. All the mapped folds are either positioned in the hanging walls of extensional (sometimes inverted) master faults or are dissected by younger faults with minor throws.

Strike-slip systems and analogue shear experiments

Shear margins and strike-slip systems are structurally complex and highly dynamic, so that the eventual architecture of such systems include structural elements that were not contemporaneous (e.g., Graymer et al., 2007; Crowell, 1962; 1974a,b; Woodcock & Fischer, 1986; Mousloupoulou et al., 2007; 2008). Analogue models offer the option to study the dynamics of such relations and therefore attracted the attention of early workers in this field (e.g., Cloos 1928; Riedel 1929) and have continued to do so until today. Early experimental works mostly utilized one-layer ("Riedel-box") models (e.g. Emmons 1969; Tchalenko, 1970; Wilcox et al., 1973), which were soon to be expanded by the study of multilayer systems (e.g. Faugère et al., 1986; Naylor et al., 1986; Richard et al., 294

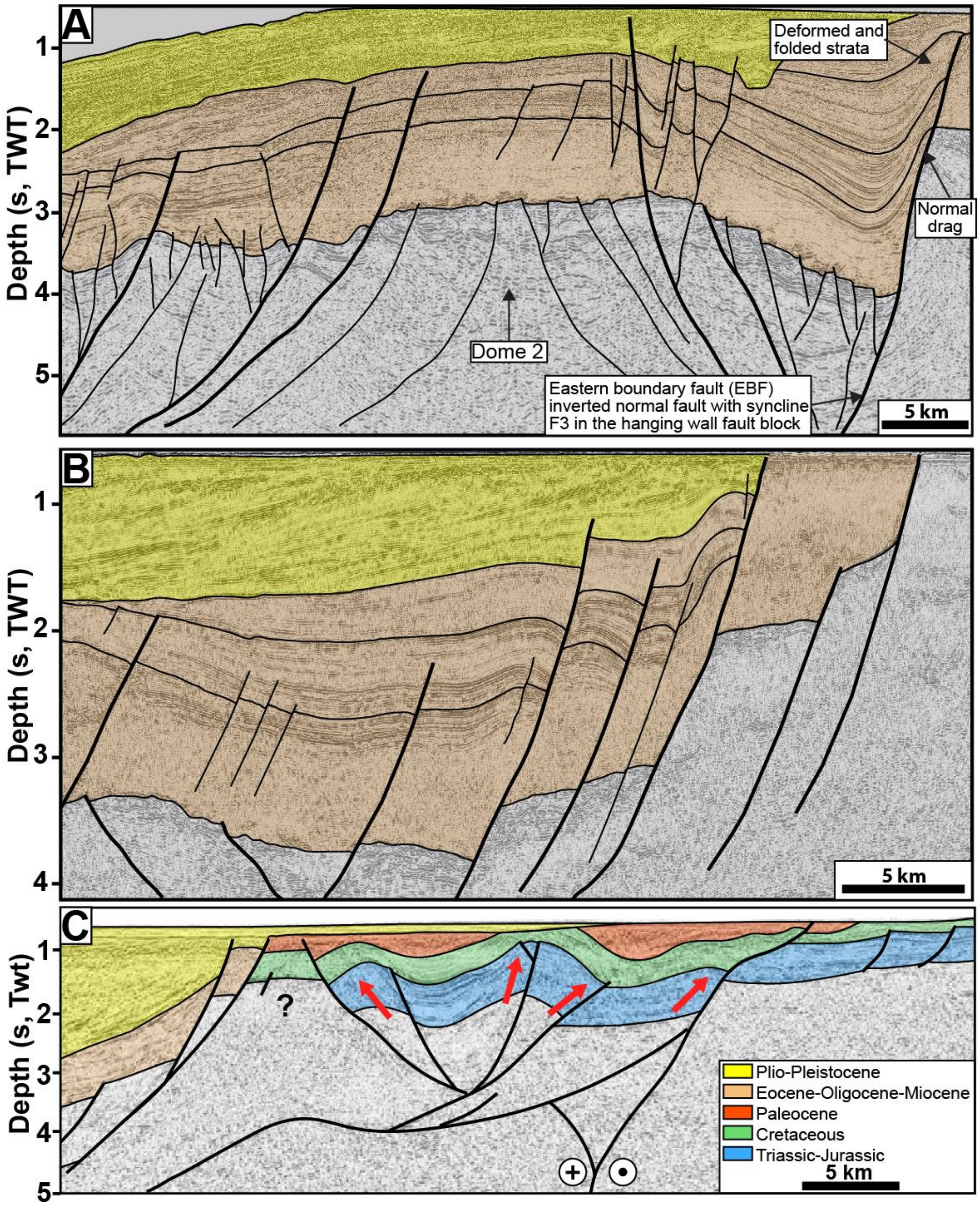
A
Depth (s, TWT)
Deformed and folded strata
Normal drag
Dome 2
Eastern boundary fault (EBF) inverted normal fault with syncline F3 in the hanging wall fault block
5 km
B
Depth (s, TWT)
5 km
C
Depth (s, Twt)
?
Plio-Pleistocene
Eocene-Oligocene-Miocene
Paleocene
Cretaceous
Triassic-Jurassic
5 km

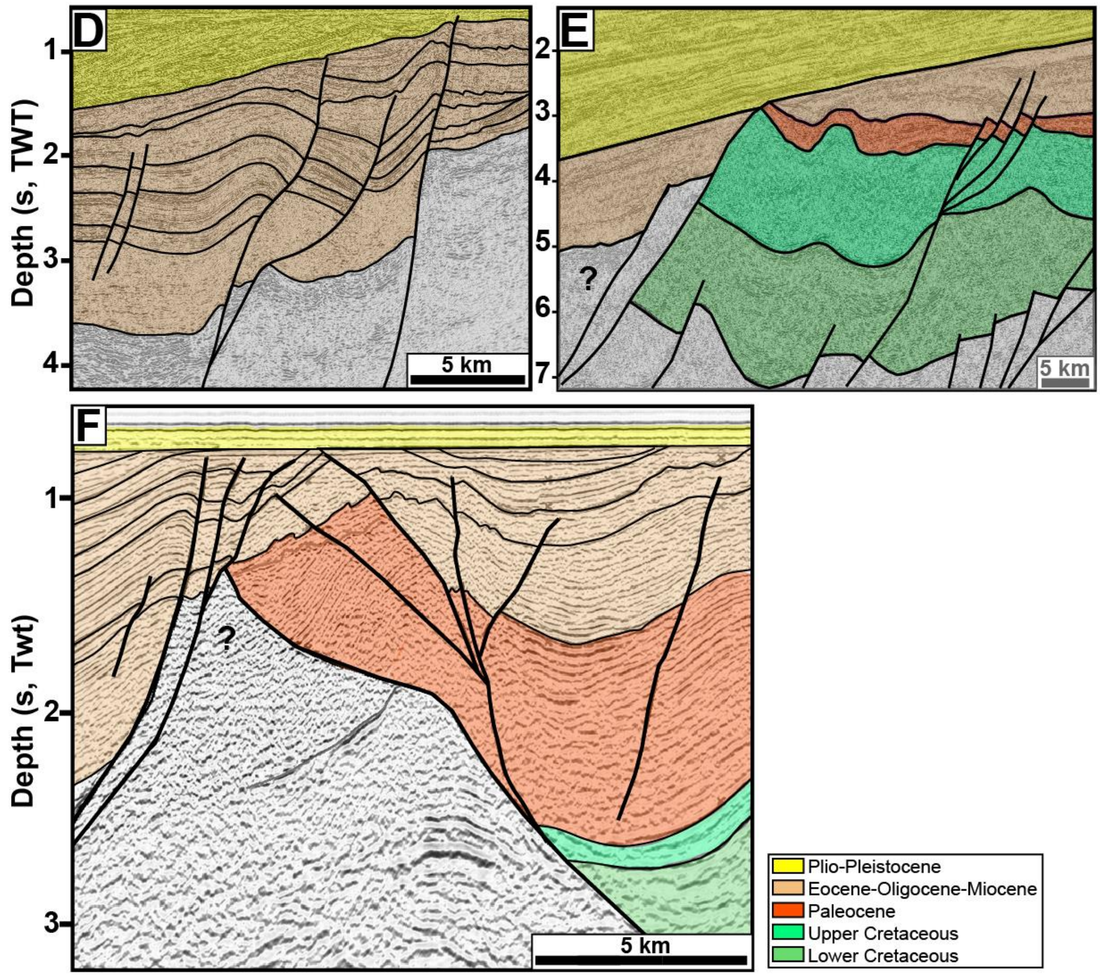

Figure 2: Seismic examples from various segments of the Barents Sea shear margin. **A)** Gentle, partly collapsed NE-SW-striking anticline/dome in the eastern terrace domain of the southern Vestbakken Volcanic Province. The origin of this structure is obscure, but one can speculate that some of the open syncline-anticline pairs originated as PSE-1-structures. **B**) Flower (PSE-2)-structure in area dominated by neutral shear. **C)** Section through push-up (PSE-4-structure) associated with restraining bend. **D-E)** Asymmetrical folds situated along the eastern margin of the Vestbakken Volcanic Province, representing primary PSE-5-structures. These structures are focused in the hangingwalls along the escarpments of master fault blocks. **F)** Trains of symmetrical folds with upright fold axes (PSE-6-structure family) are preserved inside larger fault blocks. See Table 1 and text for explanation of the PSE-structures.

1991; Richard & Cobbold, 1989, 1995; Schreurs, 1994, 2003; Manduit & Dauteuil, 1996; Dateuil & Mart, 1998; Schreurs & Colletta, 1998, 2003; Ueta et al., 2000; Dooley & Schreurs, 2012). The systematics and dynamics of strike-slip systems have been focused upon in a number of summaries like Sylvester (1985; 1988); Biddle & Christie-Blick (1985a,b); Cunningham & Mann (2007); Dooley & Schreurs (2012); Nemcok et al. (2016) and Peacock et al. (2016). Concepts and

Table 1

Characteristics of Positive Structural Elements (PSE-1 -PSE-6) as described in text and shown in figures. Note that PSE-1-structures that were developed in the earliest stages of the experiments became cannibalized or obliterated during the continued deformation. No candidates of this structure population were identified with certainty in reflection seismic sections.

Struct. type	Structural configuration	Orientation	Expr. stage	Segment	Recognized in seismic	Figure Expr	Figure Seism
PSE-1	Open syn-anticline system	135 deg	Stage 1	1,3	?	5,6	1A?
PSE-2	Incipient flower or half-flower	Parallel master fault	Stage 1	1,2,3	Yes	5,6,8	1B
PSE-3	Forced folds above rotated fault blocks	Parallel master fault in releasing bend	Stage 2	1,2	Yes	9B	
PSE-4	Push-up	Paralllel master fault in restraing bend	Stage 1	2	Yes	9D	1C
PSE-5	Anticlines/snake-heads in hanging walls	Parallel master faults	Stage 3	1,2,3	Yes	9C,D	1D,E
PSE-6	Anticline-syncline trains	Parallel master faults	Stage 3	1,2,3	Yes	12	1F

nomenclature established in these works are used in the following descriptions and analysis. Also, following Christie-Blick & Biddle (1985a,b) and Dooley & Schreurs (2012) we apply the term Principal Deformation Zone (PDZ) for the junction between the movable polythene plates underlying the experiment. The contact between the fixed and movable base defined a non-stationary velocity discontinuity ("VD"; Ballard et al., 1987; Allemand & Brun, 1991; Tron & Brun, 1991).

Several experimental studies have particularly focused on the geometry and development of pull-apart-basins in releasing bend settings (Mann et al., 1983; Faugére et al. 1983; Richard et al. 1995; Dooley & McClay 1997; Basile & Brun 1999; Sims et al., 1999; Le Calvez & Vendeville, 2002; Mann, 2007; Mitra & Paul, 2011). The pull-apart basin was described by Burchfiel & Stewart (1966) and Crowell (1974a,b) as formed at a releasing bend or at a releasing fault step-over along a strike-slip zone (Biddle & Christe-Blick 1985a,b). This basin type has also been termed "rhomb grabens" (Freund, 1971) and "strike-slip basins" (Mann et al., 1993) and is commonly considered to be synonymous with the extensional strike-slip duplex (Woodcock & Fischer, 1986; Dooley & Schreurs, 2012). In the descriptions of our experiments, we found it convenient to distinguish between extensional strike-slip duplexes in the context of Woodcock & Fischer (1986) and Twiss & Moores, 2007, p. 140-141;) and pull-apart basins (rhomb grabens: Crowell, 1974a,b; Aydin & Nur, 1993) since they reflect slightly different stages in the development in our experiments (see discussion).

Experimental setup

To study the kinematics of complex shear margins, a series of analogue experiments were performed at the tectonic modelling laboratory (TecLab) of Utrecht University, The Netherlands. All experiments were built on two overlapping 1 mm thick plastic sheets (each 100 cm long and 50 cm wide) that were placed on a flat, horizontal table surface. The boundary between the underlaying movable and overlaying stationary plastic sheets had the shape of the mapped continent-ocean boundary (COB; **Figure 1B**). The moveable sheet was

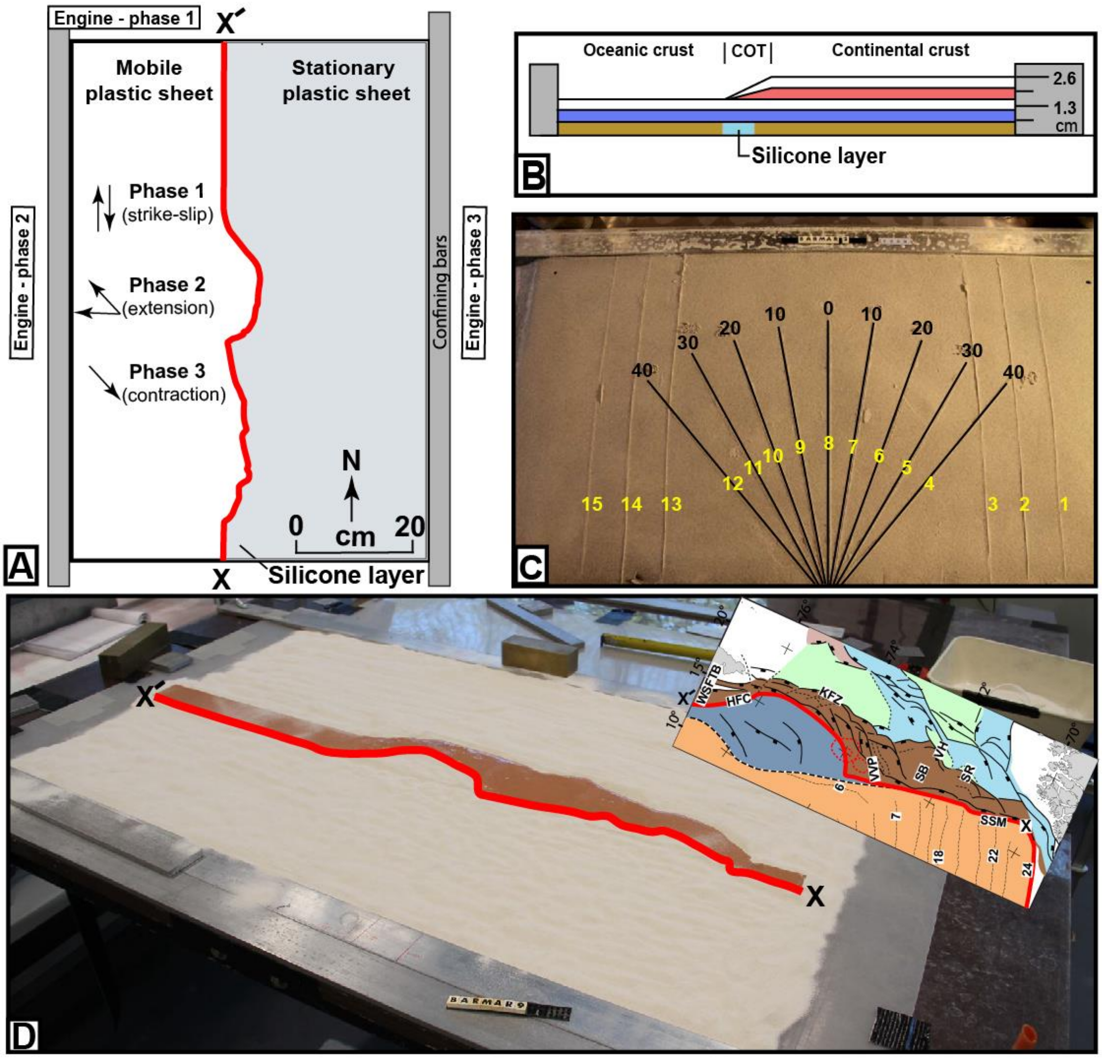

Figure 3: A) Schematic set-up of BarMar3-experiment as seen in map view. **B)** Section through same experiment before deformation, indicating stratification and thickness relations. **C)** Standard positions and orientation for sections cut in all experiments in the BarMar-series. Yellow numbers are section numbers. Black numbers indicate angle between the margins of the experiment (relative to N-S) for each profile. **D)** Outline of silicone putty layer as applied in all experiments. Inset shows original structural map of the Barents Margin used to define the width of the thinned crust (same as Fig. 1B). Red line (X-X') indicates the western limit of the thinned zone.

connected to an electronic engine, which pulled the sheet at constant velocity during all three deformation stages. Displacement rates were therefore not scaled. The modelling material was then placed on these sheets where the layers on the stationary sheet represent the continental crust including the continent-ocean transition (COT) whereas those on the mobile sheet represents the oceanic crust. The model layers were confined by aluminum bars along the long sides and sand along the short sides (**Figure 3A**). The continental crust tapers off towards the oceanic crust with a relatively constant gradient. A sand-wedge with a constant dip angle determined by the difference in thickness between the intact and the stretched crust, and that covered the width of the silicon putty layer, was made to simulate the continent-ocean transition (**Figure 3B**). The taper angle was kept constant for all models.

The pre-cut shape of the plate boundary includes major releasing bends positioned so that they correspond to the geometry of the COB and the three main structural segments of the Barents Shear Margin as follows. *Segment 1* of the BarMar-experiments (**Figure 4**) contained several sub-segments with releasing and restraining bends as well as segments of "neutral" (Wilcox et al., 1973; Mann et al. 1983; Biddle & Christie-Blick, 1985b) or "pure" (Richard et al., 1991) strike-slip. *Segment 2* had a basic crescent shape, thereby defining a releasing bend at its southern margin in the position similar to that of the Vestbakken Volcanic Province that merged into a neutral shear-segment along the strike of, whereas a restraining bend occupied the northern margin of the segment. *Segment 3* was a straight basement segment, defining a zone of neutral shear and corresponds to the strike-slip segment west of Svalbard (**Figure 1**).

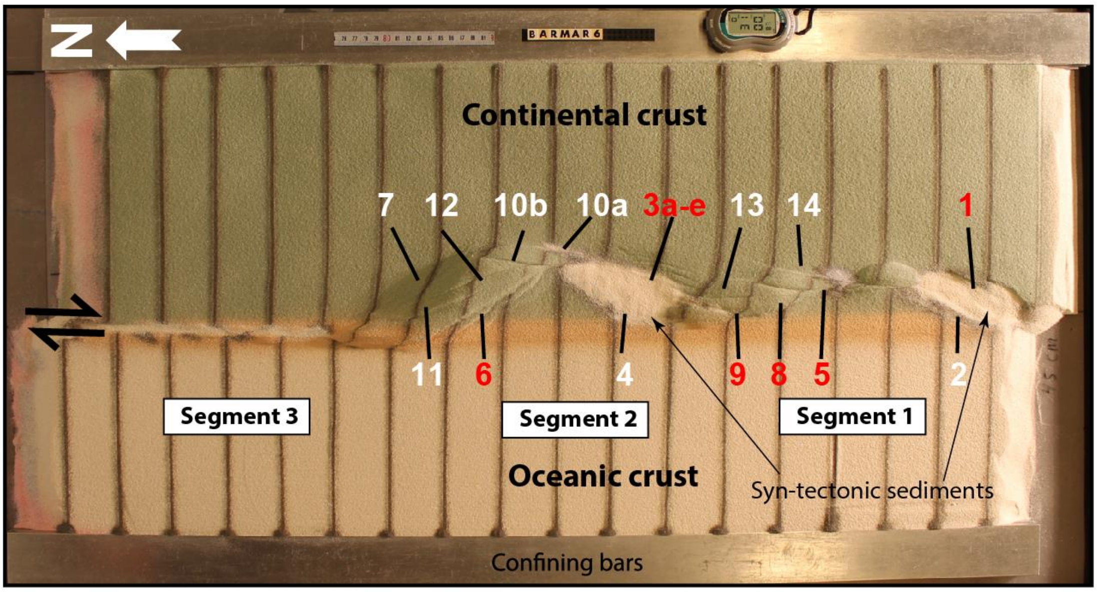

Figure 4: Position of segments and major structural elements as referred to in the text and subsequent figures (see particularly **Figures 5 and 6**). This example is taken from the reference experiment BarMar6. All experiments BarMar6-9 followed the same pattern, and the same nomenclature was used in the description of all experiments and provides the template for the definition of structural elements in Figure 7.

The experiments included three stages of deformation with constant rates of movement of the mobile sheet at 10 cmhr^{-1} in all three stages. The relative angles of plate movements in the experiments were taken from post-late Paleocene opening directions in the northeast Atlantic (Gaina et al. 2009). Dextral shear was applied in the *first phase* in all experiments by pulling the lower plastic sheet by 5 cm. In the *second phase* the left side of the experiment was extended by 3 cm orthogonally (BarMar6) or obliquely (325 degrees; BarMar 8 & 9) to the trend of the shear margin, whereas plate motion was reversed during the *third phase of deformation*, leading to inversion of earlier formed basins that had been developed in the strike-slip and extensional phases. Sedimentary basins that develop due to strike-slip (phase 1) or extension (phase 2) have been filled with layers of colored feldspar sand by sieving, so that a smooth surface was obtained. These layers are primarily important for discriminating among deformation phases and thus act as marker horizons. Phase 3 was initiated by inverting the orthogonal (BarMar6) or oblique (BarMar 8 & 9) extension of Phase 2 as a proxy for ridge-push that likely was initiated when the mid-oceanic ridge was established in Miocene time in the North Atlantic (Moser et al., 2002; Gaina et al., 2009). Contraction generated by ridge-push has been inferred from the mid-Norwegian continental shelf (Vågnes et al., 1998; Pascal & Gabrielsen, 2001; Faleide et al., 2008; Gac et al., 2016) and seems still to prevail in the northern areas of Scandinavia (Pascal et al., 2005), although far-field compression generated by other processes have been suggested (eg. Doré & Lundin, 1996).

Coloured layers of dry feldspar sand represent the brittle oceanic and continental crust. This material has proven suitable for simulating brittle deformation conditions (Willingshofer et al., 2005; Luth et al., 2010; Auzemery et al., 2021) and is characterized by a grain size of 100-200 µm, a density of 1300 kgm^{-3}, a cohesion of ~16-45 Pa and a peak friction coefficient of 0.67 (Willingshofer et al., 2018). Additionally, a 8 mm thick and of variable width corresponding to the COT (as mapped in reflection seismic data) of 'Rhodorsil Gomme GSIR' (Sokoutis, 1987) silicone putty mixed with fillers was used as a proxy for the thinned and weakened continental crust at the continent-ocean transition (**Figure 1B and 3A,B**). This

Newtonian material (n=1.09) has a density of 1330 kgm^{-3}and a viscosity of 1.42x10^{4} Pa.s.

The experiments have been scaled following standard scaling procedures as described by Hubbert (1937), Ramberg (1967) or Weijermars and Schmeling (1986), assuming that inertia forces are negligible when modelling tectonic processes on geologic timescales (see Ramberg (1981) and Del Ventisette et al. (2007) for a discussion on this topic). The models were scaled so that 10 mm in the model approximates c. 10 km in nature yielding a length scale ratio of 1.00E^{-6}. As such, the model oceanic and continental crusts scale to 18 and 26 km in nature, respectively. A 26 km thick continental crust is a representative average for the crustal thickness east of the COT, ranging between 20 km in the SW Barents Sea and 30-32 km in the NW Barents Sea (Clark et al., 2012; Breivik et al. 2003). A thinning from 26 to 18 km across the COT is also realistic, however, the oceanic crust in the Norwegian-Greenland Sea is thinner than in the scaled model (Libak et al., 2012a,b).

The brittle crust, dry feldspar sand, deforms according to the Mohr-Coulomb fracture criterion (Horsfield, 1977; Mandl et al., 1977; McClay, 1990; Richard et al., 1991; Klinkmüller et al., 2016), whereas silicone putty promotes ductile deformation and folding. The geometry applied in the present experiments is accordingly well suited for the study of the COB/COT in the Barents Shear Margin (Breivik et al., 1998).

When complete, the experiments were covered with a thin layer of sand further to stabilize the surface topography before the models were saturated with water and cross-sections that were oriented transverse to the velocity discontinuity were cut in a fan-shaped pattern (**Figure 3C**). All experiments have been monitored with a digital camera providing top-view images at regular time intervals of one minute.

All experiments performed were oriented in a N-S-coordinate framework to facilitate comparison with the western Barents Sea area and had a three-stage deformation sequence (dextral shear – opening – closure). All descriptions and

extension compression

figures relate to this orientation. It was noted that all experiments reproduced comparable basic geometries and structural types, demonstrating robustness against variations in contrasting strength of the “continent-ocean”-transition zone, which included a zone of silicone putty with variable width below an eastward thickening sand-wedge (**Figure 3B**) and changing displacement velocities.

Modelling Results

A series of nine experiments (BarMar1-9) with the set-up described above was performed. Experiments BarMar1-5 were used to calibrate and optimize geometrical outline, deformation rate, and angles of relative plate movements and are not shown here. The optimized geometries and experimental conditions utilized for experiments BarMar6-9, of which BarMar6 and 8 (and some examples from BarMar9) are illustrated here, yielded similar results in that all crucial structural elements (faults and folds) were reproduced in all experiments as described in the text and shown in **Figure 4**. It is emphasized that the extensional basins affiliated with the extension phase (phase 2) became wider in the orthogonal (BarMar6) as compared to oblique extension experiments (BarMar 8) (**Figures 5 and 6**). Furthermore, the fold systems generated in the experiments that utilized oblique contraction of $325/145^0$ (BarMar8-9) produced more extensive systems of non-cylindrical folds with continuous, but more curved fold traces as compared to experiments with orthogonal extension/contraction (BarMar6). The fold axes generally rotated to become parallel to the (extensional) master faults delineating the pull-apart basins generated in deformation stage 1 in experiments with an oblique opening/closing angle. Examples of the sequential development is displayed in **Figures 5 and 6**) and summarized in **Figure 7**.

Elongate positive structural elements with fold-like morphology as seen on the surface were detected during the various stages of the present experiments. The true nature of those were not easily determined until the experiments were terminated and transects could be examined. Such structures included buried push-ups (*sensu* Dooley & Schreurs, 2012), antiformal stacks, back-thrusts, positive flower structures, fold trains, and simple anticlines. For convenience, we use the non-genetic term “positive structural elements” termed *PSE-m-n* for such structure types as seen in the experiments in the following description. In the following the deformation in each segment is characterized for the three deformation phases **(Table 1).**

Deformation phase 1: Dextral shear stage

Segment 1: Differences in the geometry of the pre-cut fault trace between segments 1, 2 and 3 became evident after the very initial deformation stage. Particularly in segments 1 and 3 an array of oblique *en échelon* folds in between Riedel shear structures (*PSE-1-structures*) oriented c. 135° (NW-SE) to the regional VD rotating towards NNW-SSE by continued shear (**Figure 8**; see also Wilcox et al., 1973; Ordonne & Vialon, 1983; Richard et al., 1991; Dooley & Schreurs, 2012). These were simple, harmonic folds with upright axial planes and fold axial traces extending a few cm beyond the surface shear-zone described above. They had amplitudes on the scale of a few millimeters and wavelengths on scale of 5 cm. The PSE-1-structures interfered with or were dismembered by younger structures (Y-shears and PSE-2-structures; see below) causing northerly rotation of individual intra-fault zone lamellae (remnant PSE-1-structures; **Figure 8**). Structures similar to PSE-1-fold arrays are known from almost all strike-slip experiments reported and described in the literature from the early works of (eg. Cloos, 1928; Riedel, 1929. See Dooley & Schreurs, 2012 for summary) and are therefore not given further attention here.

By 0.25 cm of horizontal displacement in segment 1, which included releasing and restraining bends separated by a central strand of neutral shear, a slightly curvilinear surface trace of a NE-SW-striking, top-NW normal faults in the southernmost part of segment 1 developed. This co-existed with the PSE-1-structures and was immediately paralleled by a normal fault with opposite throw (fault 2, **Figure 4**) so that the two faults constrained a crescent- or spindle-shaped incipient extensional shear duplex (**Figures 5B and 6B**; see also Mann et al., 1983; Christie-Blick & Biddle, 1985; Mann 2007; Dooley & Schreurs, 2012).

A system of *en échelon* faults separate N-S to NNE-SSE- striking normal and shear fault segments became visible in segment 1 after ca. 1 cm of shear (**Figure 5C,D**). These faults did not have the orientations as expected for R (Riedel) - and R' (anti-Riedel)- shears (that would be oriented with angles of approximately 15 and 75° from the master fault trace) but became progressively linked by along-strike growth and the development of new faults and fault segments. They thereby acquired the characteristics of Y-shears (oriented sub-parallel to the master fault trace), dissecting the PSE-1-structures. By 2.4 cm of shear, segment 1 had become one unified fault array (**Figures 5D and 6D**), delineating a system of incipient push-ups or positive flower structures (*PSE-2-structures;* **Figures 8 and Figure 10, sections B1 and B3**, see also; Riedel, 1929; Wilcox et al., 1973; Odonne & Vialon, 1983; Dauteuil & Mart, 1995; Dooley & Schreurs, 2012).

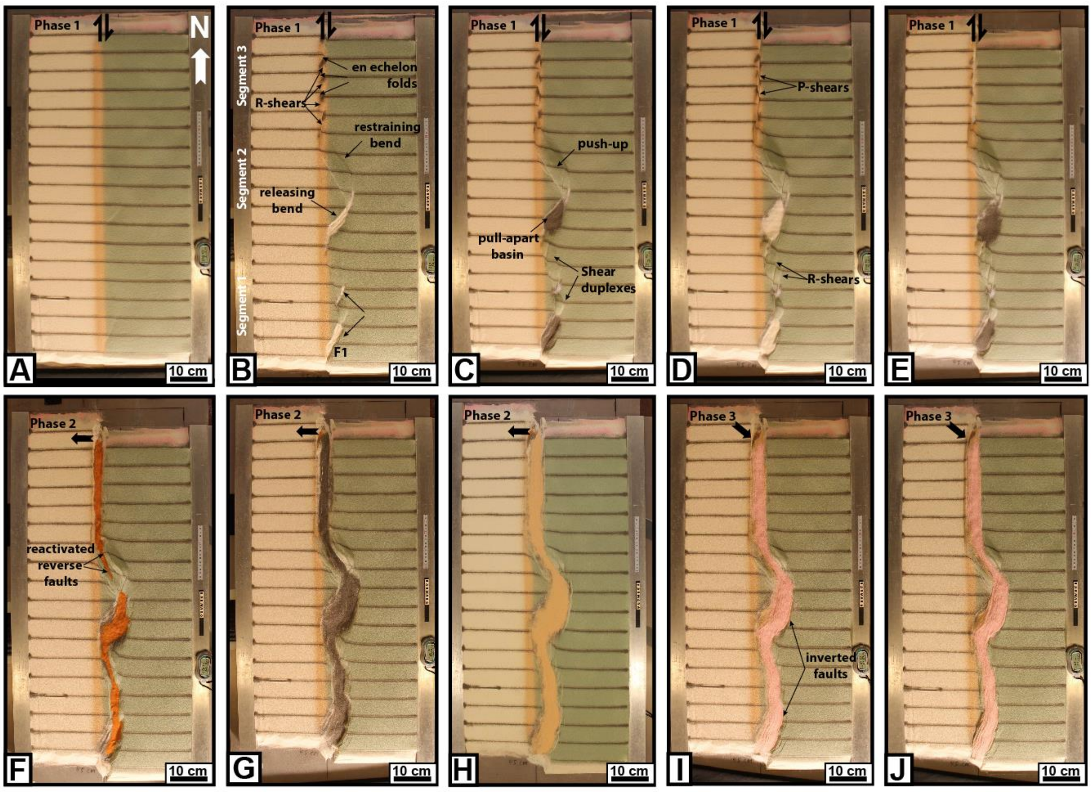

Figure 5: Sequential development of experiment BarMar6 by 0.5, 2.4, 3.5, 4.0 and 5.0 cm of dextral shear (Steps A-E), orthogonal extension (steps F-H) and oblique contraction (steps I-J). The master fault strands are numbered in **Figure 4**, and the sequential development for each structural family is shown in **Figure 7**.

The PSE-2-structures had amplitudes of 1 - 2 cm and wavelengths of 3 - 5 cm as measured on the surface with fault surfaces that steepened down-section, the deepest parts of the structures having cores of sand-layers deformed by open to tight folds. The folds had upright or slightly inclined axial planes, dipping up to 55°, mainly to the east. The structures also affected the shallowest layers down to 1-2 cm in the sequence, but the shallowest sequences were developed at a later stage of deformation and were characterized by simple gentle to open anticlines. These structures were constrained to a zone of deformation directly above the trace of the basement fault, similar to that commonly seen along shear zones (e.g. Tchalenko, 1971; Crowell, 1974 a,b; Dooley & Schreurs, 2012). This zone was 3-4 cm wide and remained stable throughout deformation stage 1 and was restricted

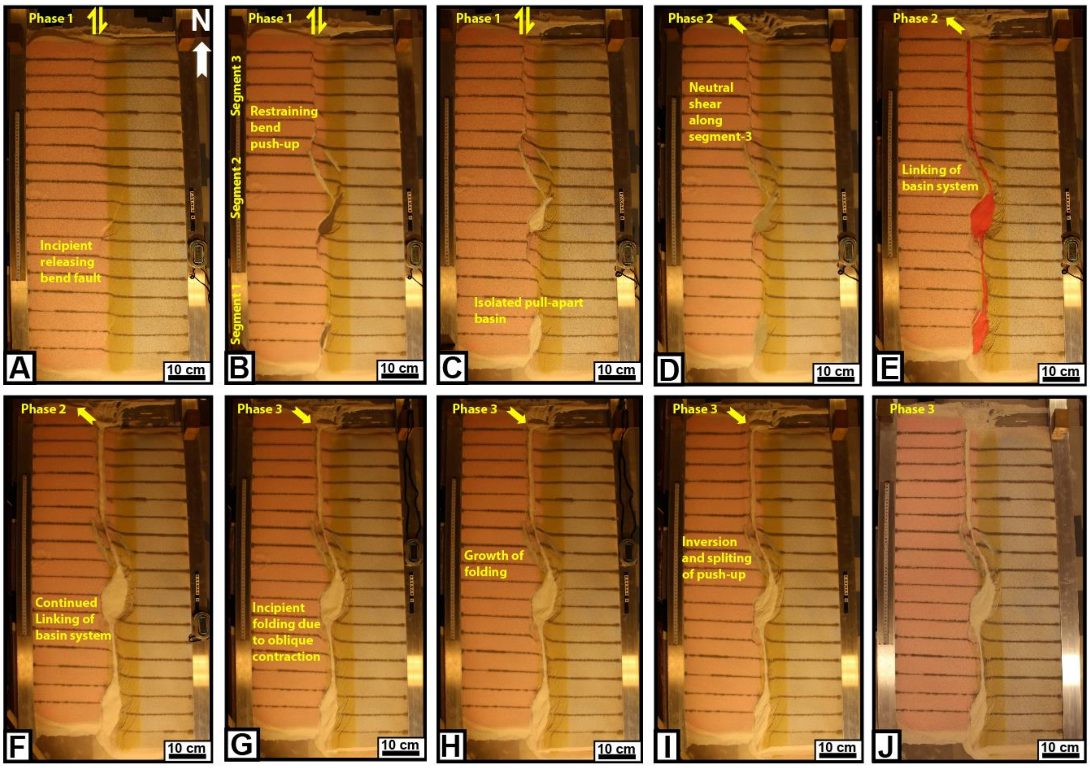

Figure 6: Sequential development of experiment BarMar8 by 1.0, 3.5 and 5.0 cm of dextral shear (Steps A-C), oblique extension (steps D-F) and oblique contraction (steps G-I). Step J represents the final model after end of contraction. The master fault strands are numbered in **Figure 3**, and the sequential development for each structural family is shown in **Figure 7**. Phases 2 and 3 involved oblique (325^0) extension and contraction in this experiment.

to the close vicinity of the basement shear fault itself as also described from one-stage shear faults in Riedel box-type experiments (e.g. Tchalenko, 1970; Naylor et al., 1986; Richard et al., 1991; Casas et al., 2001; Dauteuil & Mart, 1998; Dooley & Schreurs, 2012) and from nature as well (e.g. Wilcox et al., 1973; Harding, 1974; Harding & Lowell, 1979; Sylvester, 1988: Woodcock & Schubert, 1994; Mann, 2007).

A horse-tail-like fault array developed by ca. 3 cm of shear at the transitions between segments 1 and 2 (see also Cunningham & Mann, 2007; Dooley & Schreurs, 2012, their Figure 44) (**Figures 5B-D and 6B-D)**.
The structuring in *Segment 2;* was ruled by the crescent-shaped basement fault (VD) that generated a releasing bend along its southern and a restraining bend along its northern border (**Figure 11**). The first fault of fault array 3a-e in the southern part of Segment 2 was activated after c. 0.15 cm of bulk horizontal displacement (**Figure 7**). It was situated directly above the southernmost precut releasing bend, defining the margin of crescent-shaped incipient extensional strike-slip duplexes (in the context of Woodcock & Fischer, 1986, Woodcock & Schubert, 1994 and Twiss & Moores, 2007, p. 140-141). The developing basin got a spindle-shaped structure and developed into a basin with a lazy-S-shape (Cunningham & Mann, 2007; Mann, 2007). The basin widened towards the east by stepwise footwall collapse, generating sequentially rotating crescent-shaped extensional fault blocks that became trapped as extensional horses in the footwall of the releasing bend (**Figure 11**). In the areas of the most pronounced extension, the crestal part of the rotational fault blocks became elevated above the basin floor, generating ridges that influenced the basin floor topography and hence, the sedimentation. By continued rotation of the fault blocks and simultaneous sieving of sand the crests of the blocks became sequentially uplifted, generating forced folds (Hamblin, 1965; Stearns, 1978; Groshong, 1989; Khalil & McClay, 2016) (**Figure 10A**). In the analysis we used the term *PSE-3-structures* for these features. Simultaneously, an expanding sand-sequence became trapped in the footwalls of the master faults, defining typical growth-fault geometries.

By a shear displacement of 0.55 cm additional curved splay faults were initiated from the northern tip of the master fault of fault 3f; **Figure 7**), delineating the northern margin of a rhombohedral pull-apart-basin (Mann et al., 1983; Mann,

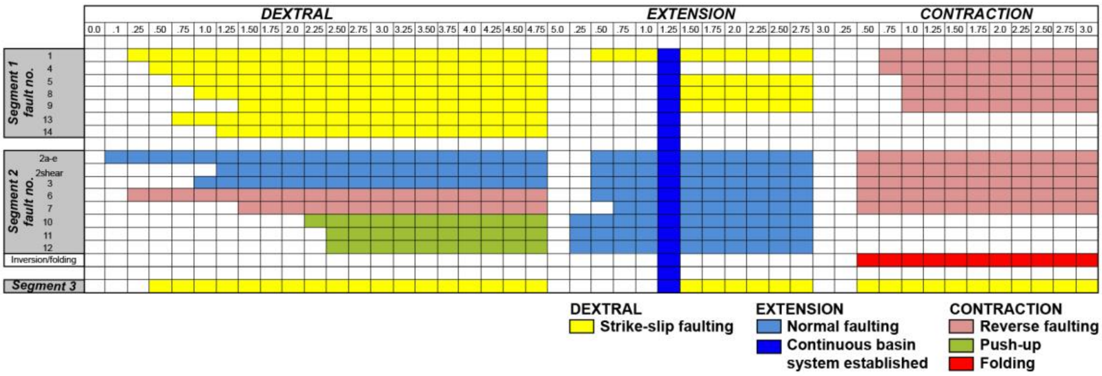

Figure 7: Summary of sequential activity in each master structural element **(Figure 4)** in Experiment BarMar6 (**Figure 5**). Type and amount of displacement is shown in two upper horizontal rows. The vertical blue bar indicates the stage at which full along-strike communication became established between marginal basins. Color code (see in-set) indicates type of displacement at any stage.

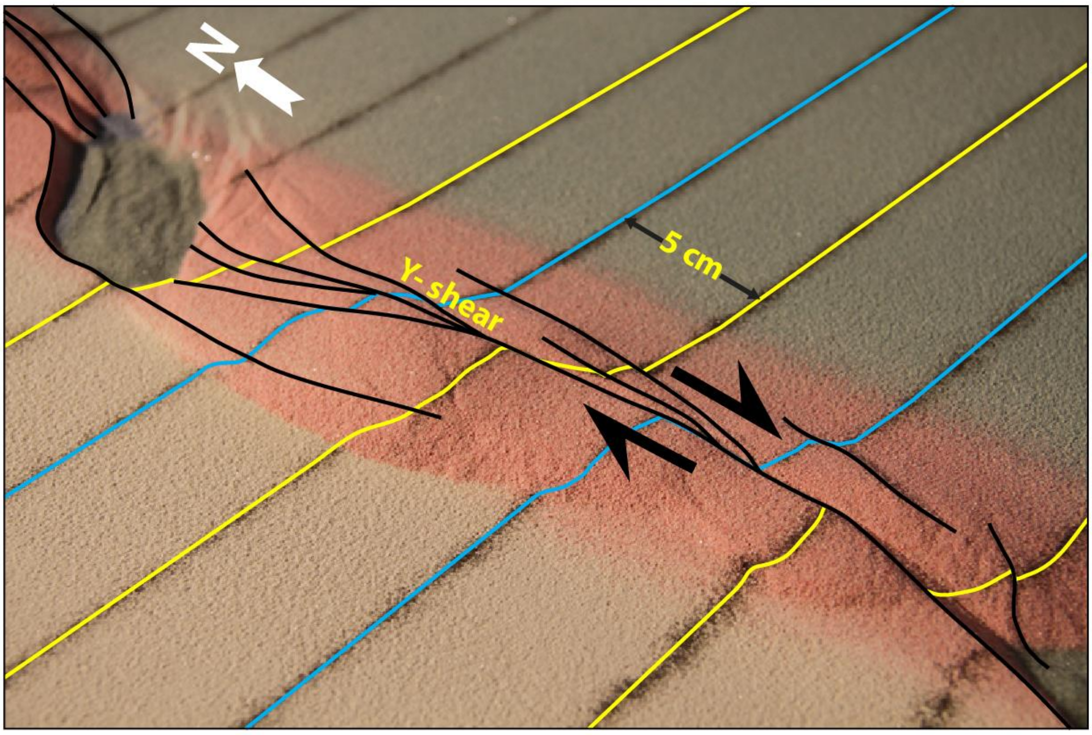

Figure 8: PSE-1 anticline-syncline pairs in segment 1 experiment BarMar6 in an oblique view. PSE-1 folds were constrained to the very fault zone and the fold axes (blue lines) and extended only 3-4 cm beyond the fault zone. PSE-2 structures (incipient shear-duplex and positive flower structures; yellow lines) were delineated by shear faults and completely cannibalized PSE-1 structures by continued shear. Yellow and blue lines show the rotation of the fold axial trace caused by dextral shearing of c. 1,5 cm. 25mm of dextral shear. By a displacement of 35mm the remains of the PSE-1 structure was completely obliterated. The distance between the markers (dark lines) is 5cm. Yellow arrow marks north-direction. White arrows indicate shear direction.

2007; Christie-Blick & Biddle, 1985) and with a geometry that was indistinguishable from pull-apart basins or rhomb grabens affiliated with unbridged *en échelon* fault arrays (Crowell, 1974 a,b; Aydin & Nur, 1993). Although sand was filled into the subsiding basins to minimize the graben relief and to prevent gravitational collapse, the sub-basins that were initiated in the shear-stage were affected by internal cross-faults, and the initial basin units remained the deepest so that the buried internal basin topography maintained a high relief with several apparent depocenters separated by intra-basinal platforms.

Systems of linked shear faults and PSE-structures became established in the central part with neutral shear that separate the releasing and restraining bends and development similarly to that seen for segment 3 (see below). However, these structures were soon destroyed by the combined development of the northern and southern tips of the extensional and contractional shear duplexes (**Figure 10**).

The first structure to develop in the regime of the restraining bend (segment 2; was a top-to-the-southwest (antithetic) thrust fault at an angle of 145^0 with the regional trend of the basement border as defined by segments 1 and 3 (Fault 6). It became visible by 0.5 cm of displacement. The northern part of segment 2 became, however, dominated by a synthetic contractional top-to-the-northeast fault that was initiated by 0.85 cm of shear (Fault 7; **Figures 5 and 6**). Thus, faults 6 and 7 delineated a growing half-crescent-shaped 5-7-cm wide push-up structure (Aydin & Nur, 1982; Mann et al., 1983) south of the restraining bend (**Figure 9**; *PSE-4-structures*). By continued shear these structures got the character of an antiformal stack.

Segment 3 defined a straight strand of neutral shear. Its development in the BarMar-experiments followed strictly that known from numerous published experiments (e.g., Tchalenko, 1970; Wilcox et al., 1973; Harding, 1974; Harding & Lowell, 1979; Naylor et al., 1986; Sylvester, 1988; Richard et al., 1991; Woodcock & Schubert, 1994; Dauteuil & Mart, 1998; Mann, 2007; Casas et al., 2001; Dooley

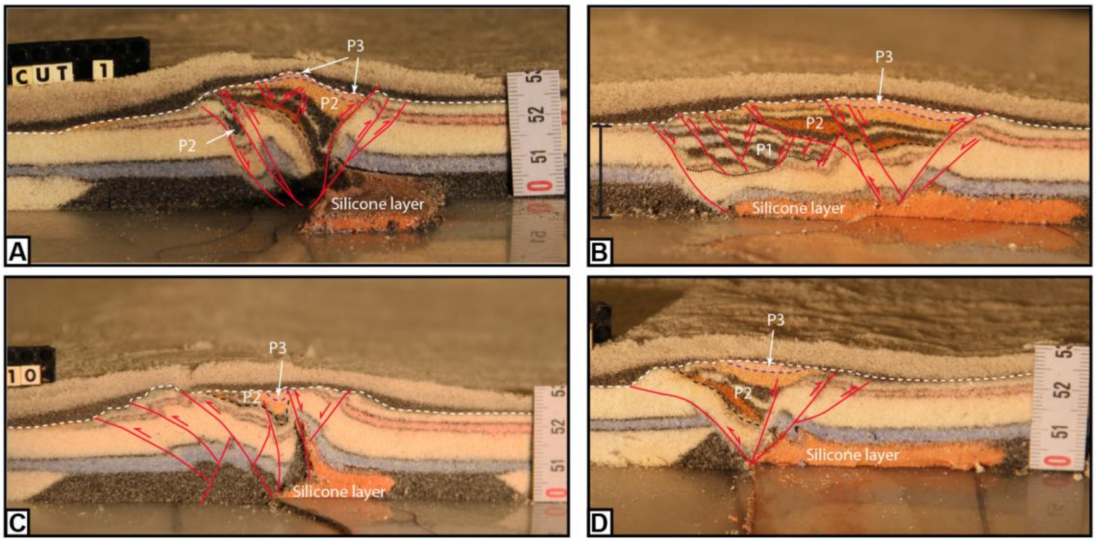

Figure 9: Cross-sections through PSE-2-related structures. **A)** Folded core of incipient push-up/positive flower structure in segment 1, experiment BarMar6. The fold structure is completely enveloped of shear faults that have a twisted along-strike geometry. Note that the eastern margin of the structure developed into a negative structure at a late stage in the development (filled by black-pink sand sequence) and that the silicone putty sequence (basal pink sequence) was entirely isolated in the footwall. **B)** Similar structure in experiment BarMar8. The weak silicone putty layer here bridged the high-strain zone and focused folding that propagated into the sand layers (blue). The folds in upper (pink layers) were associated with the contraction stage, because they contributed to a surface relief filled in by red-black-sand sequence that was sieved into the margin during the contraction stage. **C)** Contraction associated with "crocodile structure" in the footwall of the main fault in segment 1, experiment BarMar8. Note disharmonic folding with contrasting fold geometries in hanging wall and footwall and at different stratigraphic levels in the footwall, indicating shifting stress situation in time and space in the experiment. **D)** Transitional fault strand between to more strongly sheared fault segments (experiment BarMar9).

& Schreurs, 2012). A train of Riedel-shears, occupying the full length of the segment, appeared simultaneously on the surface after a shear displacement of 0.5 cm, occupying a restricted zone with a width of 2-3 cm. The Riedel-shears dominated the continued structural development of Segment 3. Riedel'-shears were absent throughout the experiments, as should be expected for a sand-dominated sequence (Dooley & Schreurs, 2012). P-shears developed by continued shear, creating linked rhombic structures delineated by the Riedel- and P-shears generating positive structural elements with NW-SE- and NNE-SSE-striking axes (see also Morgenstern & Tchalenko, 1967), soon coalescing to form Y-shears. Transverse sections document that these structures were cored by push-up

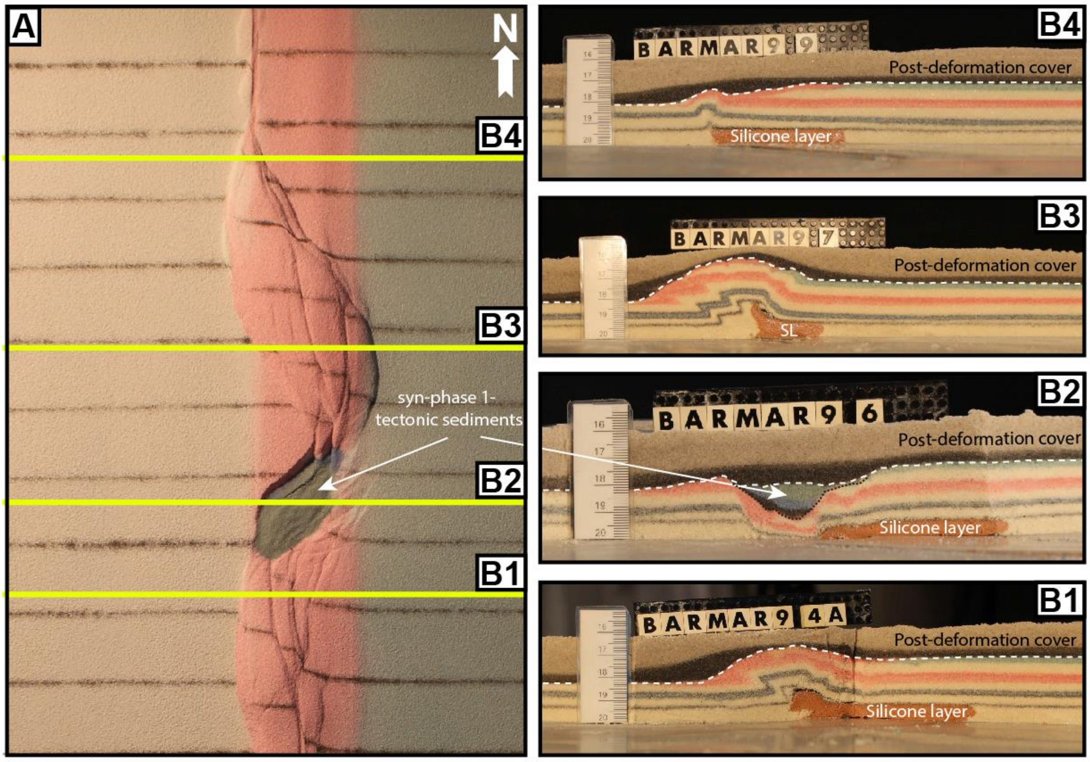

Figure 10: A) contrasting structural styles along the master fault system in segment 2 in map view and **(B)** cross sections of experiment BarMar9. SL denotes silicone layer, the stippled line the boundary between pre-and syn-deformation layers and the white dashed line the boundary with the post-deformation layers.

anticlines, positive half-flower structures and full-fledged positive flower structures in the advanced stages of shear (*PSE-4-structures*) (**Figures 5 and 6. See also Figure 10**). These were accompanied by the development of *en échelon* folds and flower structures as commonly reported from strike-slip faults in nature and in experiments. The width of the zone above the basal fault remained almost constant throughout the experiments, but was somewhat wider in experiments with thicker basal silicone polymer layers, similar to that commonly described from comparable experiments (eg., Richard et al., 1991).

Deformation Phase 2: Extension

The Palaeogene dextral shear was followed by pure extension accompanying the opening along the Barents Shear Margin in the Oligocene. Our experiments focused on the effects of oblique extension, acknowledging that plate tectonic

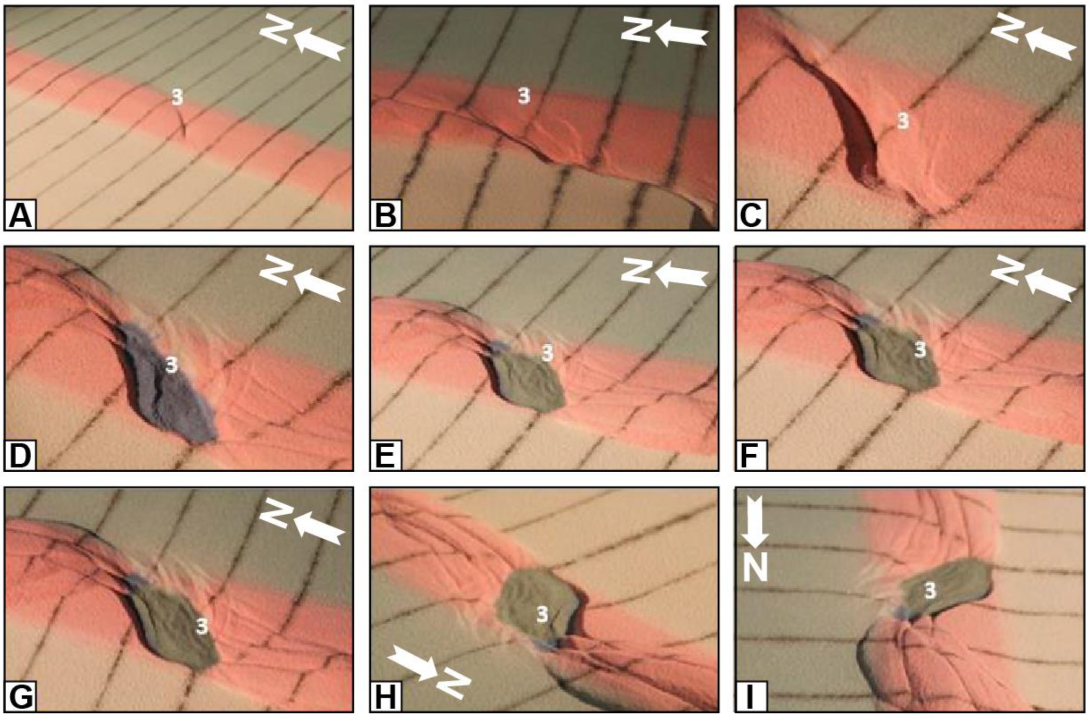

Figure 11: Nine stages in the development of the extensional shear duplex system above the releasing bend in experiment BarMar9. The master faults that developed at an incipient stage (e.g., Fault 3 that constrained the eastern margin of the extensional shear duplex) remained stable and continued to be active throughout the experiment (Figure 7), but became overstepped by faults in its footwall that became the basin contraction faults at the later stages H and I. Note that the developing basement was stabilized by infilling of gray sand during this part of the experiment. Note that Fault 3 remained active and broke through the basin infill also after the basin infill overstepped the original basin margin. The distance between the markers (dark lines) is 5cm. Yellow arrow marks north-direction. Note that figure I has a different orientation.

reconstructions of the North Atlantic suggest an extension angle of 325^{o} as the most likely (Gaina et al., 2009).

All strike-slip basins widened in the extensional stage, and most extensively so for the experiments with orthogonal extension. The widening of the basin enhanced the topography already generated in the shear-stage in the extensional strike-slip duplex in segment 2 (PSE-3-structures). In the earliest extensional stage the strike-slip basin in segment 2 dominated the basin configuration, but by continued extension the linear segments and the minor pull-apart basins in segments 1 and 2 started to open and became interlinked, subsequently generating a linked basin system that paralleled the entire shear margin (**Figures 5F-G, 6F-G**).

The extension-phase following dextral strike-slip reactivated and very quickly linked several of the master faults that were established in deformation phase 1 (**Figures 5A and 6A**) already by an extension of 0,25 – 0,50 cm. This included the southern fault margin, the push-up and the splay faults defining a crestal collapse graben of the push-up (Faults 6, 11 and 12; **Figure 4**). All three segments were reactivated in extension by c. 1.25 cm of orthogonal stretching (**Figure 7**). During the first cm of extension each basin remained an isolated unit, but after 1 cm of extension all basins became linked, thus forming one unified elongate extensional basin (marked by the vertical dark blue line in **Figure 7**) and mainly following the PDZ as it was cut in the basal templates. Among the faults that were inactive and remained so throughout the extension phase were the antithetic contractional fault delineating the push-ups in segment 2 towards the south (Fault 6; **Figure 4**). The Y-shear in Segment 3 was reactivated as a straight, continuous extensional fault in Stage 2. Total extension in Phase 3 was 5 cm.

Deformation Phase 3: Contraction

In our experiments the extension stage was followed by orthogonal or oblique contraction (parallel to the direction of extension as applied for each experiment). The experiments were terminated before the full closure of the basin system, in accordance with the extension vector > contraction vector as in the North Atlantic (see Vågnes et al., 1998; Pascal & Gabrielsen 2001; Gaina et al. 2009). A part of the early-stage contraction was accommodated along new faults. It was more common, however, that faults that had been generated in the strike-slip and extensional stages became reactivated and rotated, and the development of isolated folds, which were commonly associated with inverted fault traces, generating snakehead- or harpoon-type structures (Cooper et al., 1989; Coward, 1994; Allmendinger, 1998; Yameda & McClay, 2004; Pace & Calamitra, 2014); *PSE-5-stuctures*). This was particularly the case for the master faults. The dominant structures affiliated with the contractional stage was still new folds with traces oriented orthogonal to the shortening direction and sub-parallel to the preexisting master fault systems that defined the margin and basin margins (**Figure 12**). Also,

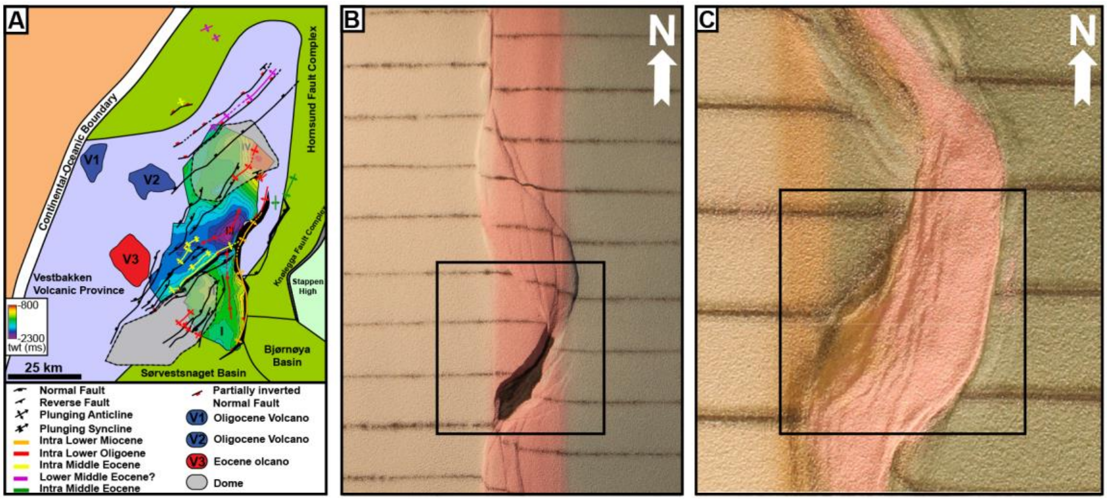

Figure 12: PSE-5 and PSE-6 folds generated during phase 3-inversion, experiment BarMar8. Note that fold axes mainly parallel the basin rims, but that they deviate from that in the central parts of the basins in some cases. Note that the folds are best developed in segment 2, which accumulated extension in the combined shear and extension stages.

some deep fold sets that had been generated during the strike-slip phase and seen as domal surface features became reactivated, causing renewed growth of surface structures (see **Figure 10** and explanation in figure caption). These folds were generally up-right cylindrical buckle folds in the initial contractional stage and with very large trace length: amplitude-ratio (*SPE-6-structures*). Some intra-basin folds, however, defined fold arrays that diagonally crossed the basins. Particularly the folds situated along the basin margins developed into fault propagation-folds above low-angle thrust planes. Such faults aligning the western basin margins could have an antithetic attitude relative to the direction of contraction.

During the contractional phase the margin-parallel, linked basin system started immediately to narrow and several fault strands became inverted. The basin-closure was a continuous process until the end of the experiment by 3 cm of contraction. The contraction was initiated as a proxy for an ESE-directed ridge-push stage. The first effect of this deformation stage was heralded by uplift of the margin of the established shear zone that had developed into a rift during deformation stage 2. This was followed by the reactivation and inversion of some master faults (e.g., fault a2; **Figure 4**) and thereafter by the development of a new set of low-angle top-to-the-ESE contractional faults. These faults displayed a sequential development (**Figure 4**) and were associated with folding of the strata in the rift structure, probably reflecting foreland-directed in-sequence thrusting (PSE-5 and PSE-6 fold populations).

Discussion

The break-up and subsequent opening of the Norwegian-Greenland Sea was a multi-stage event (**Figure 13**) that imposed shifting stress configurations overprinting the already geometrically complex Barents Shear Margin. Therefore, scaled experiments were designed to illuminate the structural development of the Barents Shear Margin. The experiments utilized three main segments that correspond to the Senja Fracture Zone (segment 1), the Vestbakken Volcanic Province (segment 2) and the Hornsund Fault Zone (segment 3). A series of structural families developed during the experiments, most of which correspond to structural elements found along the Barents Shear Margin.

Segment 1 in the experiments (which correponds to the Senja Shear Margin) was dominated by neutral dextral shear, although subordinate jogs in the (pre-cut) fault provided minor sub-segments with mainly releasing and subordinate restraining bends. PSE-1-folds that developed at an incipient stage were immediately paralleled by two sets of normal faults with opposite throw in the releasing bend areas (e.g., fault 2; **Figure 4**). The two faults defined a crescent- or spindle-shaped incipient extensional shear duplex (**Figures 5B and 6B**; see also Mann et al., 1983; Christie-Blick & Biddle, 1985; Mann, 2007; Dooley & Schreurs, 2012). The most prominent of these structures corresponds to the position of the Sørvestsnaget Basin (**Figure 1B**).

Counterparts to PSE-1 and PSE-2 structural populations observed in the experiments were not identified with certainty in the seismic data along the Barents Shear Margin, although some isolated, local anticlinal features could be dismembered remnants of such. The PSE-1 and PSE-2 structures generally belong to the structural populations that were developed at the earliest stages of the experiments. Furthermore, these structure types were confined to the area just

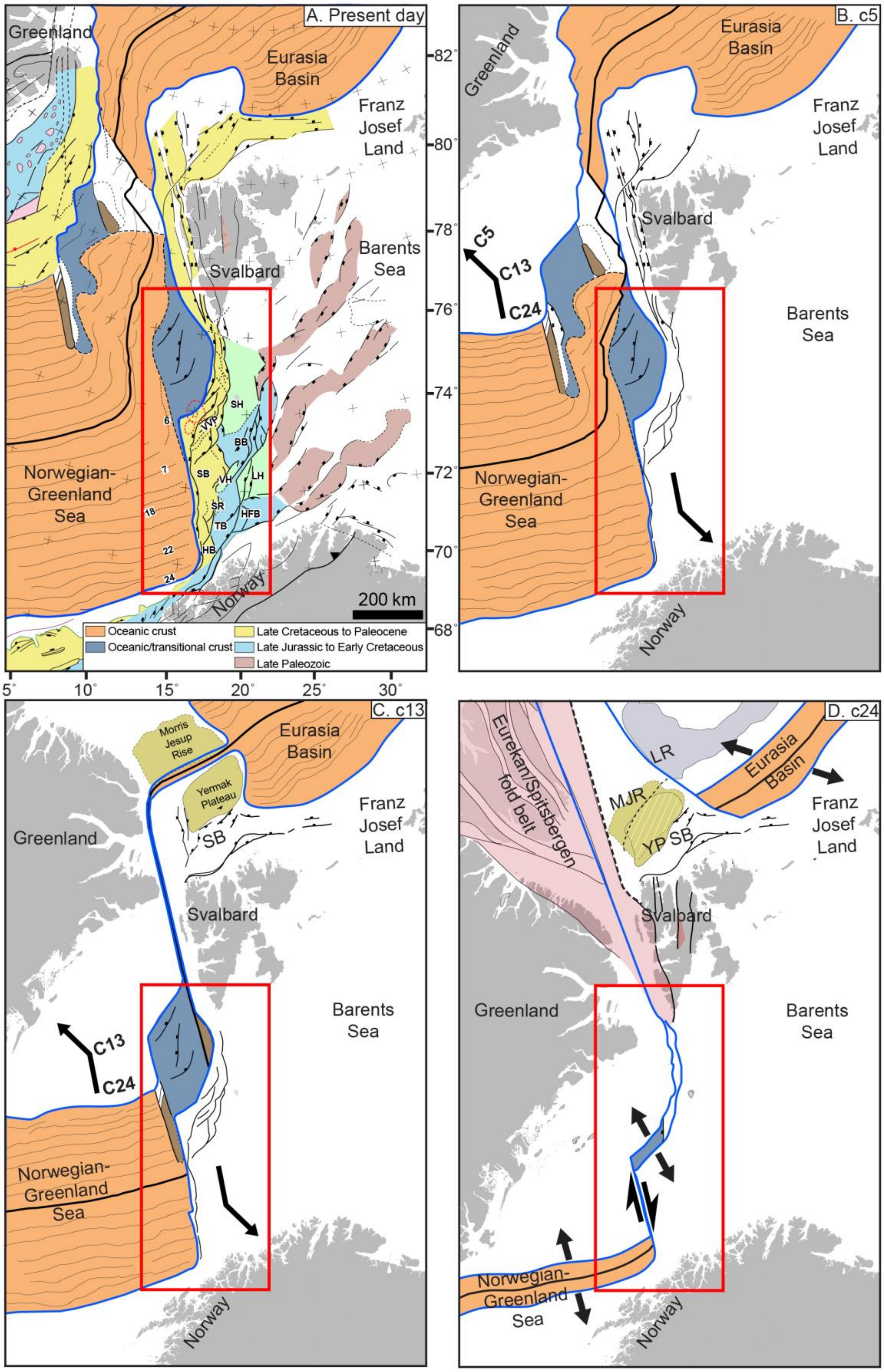

Figure 13; Main stages in opening of the North Atlantic. A) Present day, B) chron 5 (10 Ma in the late Miocene), C) chron 13 (33 Ma in the earliest Oligocene), D) chron 24 (53 Ma in the early Eocene).

above the basal master fault (VD) and its immediate vicinity (see also experiments in series "e" and "f" of Mitra & Paul, 2011). Because of their constriction to the near vicinity of the master fault, we speculate that structures generated at an early stage of shear, are vulnerable to canabalisation by younger structures with axes striking parallel to the main shear fault (Y-shears; SPE-2-structures). We therefore conclude that the majority of these structure populations were destroyed during the later stages of shear and during the subsequent stages of extension and contraction.

During the oblique extension stage segment 1 of experiments BarMar7-9 the basin subsidence was focused in the minor pull-apart basins, which soon became linked along the regional N-S-striking basin axis. Remains of several such basin centers, of which the Sørvestsnaget Basin (Knutsen & Larsen, 1997; Kristensen et al., 2017) is the largest, are preserved and found in seismic data (**Figure 1b**). During the experiments a continuous basin system was developed in the hangingwall side of the master fault, but it is not likely that opening occurred prior to the extension of the margin underlain by continental crust reached a stage where the separate basin units paralleling the Barents Shear Margin became linked.

In the subsequent inversion stage, fold trains with axial traces parallel (PSE-5-folds) to the basin axis and the master faults characterized segment 1. Remnants of such folds are locally preserved in the thickest sedimentary sequences affiliated with the Senja Shear Margin.

Segment 2, which was underlain by a crescent-shaped discontinuity corresponds to the Vestbakken Volcanic Province and the southern extension of the Knølegga Fault Complex that is a branch of the southern part of the Hornsund Fault Zone (**Figures 1b and 4**). The part of the Vestbakken Volcanic Province that was the subject of structural analysis by Giennenas (2018) corresponds to the southern part of segment 2 in the present experiments. It is dominated by interfering NNW-SSE- and NE-SW striking fold- and fault systems in the central part of the basins, whereas N-S-structures are more common along its eastern margin (**Figure 12A**) (Jebsen & Faleide, 1998; Giennenas, 2018).

Intra-basinal platforms and complex internal configurations seen in the BarMar-experiments are common in strike-slip basins (eg. Dooley & McClay, 1997; Dooley & Schreurs, 2012) and are consistent with the structural configuration with intra-basin depo-centers within the Vestbakken Volcanic Province and also in the Sørvestsnaget Basin (Knutsen & Larsen, 1997; Jebsen & Faleide, 1998; **Figure 13**). The positive structural elements that prevail in *segment 3* belong to the PSE-2-structure population. The structures affiliated with segment 3 in the BarMar-experiments are similar to those seen in the reflection seismic sections along parts of the Spitsbergen and the Senja shear margins (Myhre et al., 1982; Faleide et al., 1993). Thus, the structuring in the segment 3 in the BarMar-experiments display a configuration typical for neutral shear (Cloos, 1928; Riedel, 1929; Tchalenko, 1970; Wilcox et al., 1973). *Én echelon* folds (corresponding to PSE-1-structueres) first became visible, to be succeeded by the development of Riedel- and P-shears (R'-shears were subdued as expected for sand-dominated sequences (Dooley & Schreurs, 2012). Continued shear followed by collapse and interaction between Riedel and P-shears and the subsequent development of Y-shears initiated push-up- and flower-structures with N-S-axes (PSE-2), structures that were expressed as non-cylindrical (double-plunging) anticlines on the surface (e.g., Tchalenko, 1970; Naylor et al., 1986). Structures similar to the PSE-2-structures that were initiated in the present experiments have previously been reported from similar experiments with viscous basal layers covered by sand (e.g. Richard et al., 1991; Dauteuil & Mart, 1998), illustrating the influence of a mechanical stratified sequence on fold configurations.

The Knølegga Fault Zone occupies a km-wide zone. The master fault strand is paralleled by faults with significant normal throws on its hanging wall side and this is considered to be strands belonging to the larger Knølegga Fault Complex (EBF; Eastern Boundary Fault; Giannenas, 2018; **Figure 12A**). The EBF zone is a top-west normal fault with maximum throw of nearly 2000 ms (3000 meters). It can be followed along its strike for more than 60 km and seems to die out by horse-tailing at its tip-points. The vicinity of the master faults of the Knølegga Fault Complex locally display isolated elongate positive structures constrained by steeply dipping faults. These structures sometimes display internal reflection patterns that seem exotic or suspect in comparison to the surrounding sequences. Some of these structures resemble positive flower structures or push-ups or define narrow anticlines. They are found in both the footwall and hanging wall of the border faults and strike parallel to those and the axes of these structures parallel the master faults. The traces of such structures can be followed over shorter distances than the master faults, and do not occur in the central parts of the Vestbakken Volcanic Province. We speculate that these are rare fragments of dismembered PSE-1-type structures.

Due to the right-stepping geometry during dextral shear in segment 2, the southern and northern parts were in the releasing and restraining bend positions, respectively (e.g., Christie-Blick & Biddle, 1985). Hence, the southern part of segment 2 was subject to oblique extension, subsidence and basin formation when the northern part was subject to oblique contraction, shortening and uplift. The southern segment expanded to the east and northeast by footwall collapse and activation of rotating fault blocks that contributed to a basin floor topography that affected the pattern of sediment accumulation (**Figure 9A, B**). The crests of the rotating fault blocks are termed PSE-3-structures above, and such eroded fault block crests are defining the footwalls of major faults in the Vestbakken Volcanic Province, providing space for sediment accumulation in the footwalls. The area that was affected by the basin formation in the extensional shear duplex stage seems to have remained the deepest part of the Vestbakken Volcanic Province, whereas the part formed in basin widening by sequential footwall collapse created a shallower sub-platform (*sensu* Gabrielsen, 1986) (**Figure 11**). It is expected that (regional) basin and (local) fault block subsidence became accelerated during phase 2 (extension), and more so in the orthogonal extension experiments (BarMar 6) than in the experiments with oblique extension (BarMar 8), but due to stabilization of basins by infilling of sand, this was not documented. The widening occurred mainly by fault-controlled collapse of the footwalls, and dominantly along the master faults that correspond to the Knølegga Fault Zone, but also new intra-basin cross-faults that were initiated in the shear stage (see above) became reactivated, contributing to the complexity of the basin topography. It is not likely that a stage was reached where all (pull-apart) basin units along the margin became fully linked, although sedimentary communication along the margin may have become established.

The contraction (phase 3) clearly reactivated normal faults, probably causing focusing of hanging wall strain and folding, rotation of fault blocks and steepening of faults. This means that both intra-basinal and marginal faults in the Vestbakken Volcanic Province can have suffered late steepening. Contraction expressed as fold systems with fold axes paralleling the basin margins development seems to correspond very well to the observed structural configuration of the Vestbakken Volcanic Province. Here pronounced tectonic inversion is focused along the N-S-striking basin margins and along some NE-SW-striking faults in the central parts of the basin. Pronounced shortening also occurred inside individual reactivated fault blocks either by bulging of the entire sedimentary sequence or as trains of folds (**Figure 12**).

The restraining bend configuration in the northern part of segment 2 was characterized by increasing contraction across strike-slip fault strands that splayed out to the northwest from the central part of segment 2 in an early stage of dextral shear. This deformation was terminated by the end of phase 1 by stacking of oblique contraction faults (PSE-5 and PSE-6-structures), defining an antiformal stack-like structure. This type of deformation falls outside the main area, but to the north this type of oblique shortening during the Eocene (phase 1) was accommodated by regional-scale strain partitioning (Leever et al., 2011a,b).

The Vestbakken Volcanic Province is characterized by extensive regional shortening. Onset of this event of inversion/contraction is dated to early Miocene (Jebsen & Faleide, 1998, Giennenas, 2018) and this deformation included two main structural fold styles. The first includes upright to steeply inclined closed to open anticlines that are typically present in the hanging wall of master faults. These folds typically have wavelengths in the order of 2.5 to 4.5 kilometers, and amplitudes of several hundred meters. Most commonly they appear with head-on snakehead-structures and are interpreted as buckle folds, albeit a component shear may occur in the areas of the most intense deformation, giving a snake-head-type geometry. The second style includes gentle to open anticline-syncline pairs with upright or steep to inclined axial planes with wavelengths in the order of 5 to 7 kilometers and amplitudes of several tens of meters to several hundred meters. We associate those with the PSE-4-type structures as defined in the BarMar-experiments. These folds are situated in positions where sedimentary sequences have been pushed against buttresses provided by master faults along the basin margins. The PSE-6 folds developed as fold trains in the interior basins, where buttressing against larger fault walls was uncommon. Also, this pattern fits well with the development and geometry seen in the BarMar-experiments, where folding started in the central parts of the closing basins before folding of the marginal parts of the basin. In the closing stage the folding and inversion of master faults remained focused along the basin margins.

The experiments clearly demonstrated that contraction by buckle folding was the main shortening mechanism of the margin-parallel basin system generated in phase 2 (orthogonal or oblique extension) in all segments. In the Vestbakken Volcanic Province segments of the Knølegga Fault Zone, the EBF and the major intra-basinal faults contain clear evidence for tectonic inversion, whereas this is less pronounced in others. The hanging wall of the EBF is partly affected by fish-hook-type inversion anticlines (Ramsey & Huber, 1987; Griera et al., 2018) (**Figure 2D, E**), or isolated hanging wall anticlines or pairs or trains of synclines and anticlines (e.g., Roberts, 1989; Coward et al., 1991; Cartwright, 1989; Mitra, 1993; Uliana et al., 1995; Beauchamp et al. 1996; Gabrielsen et al. 1997; Henk & Nemcok 2008), the fold style and associated faults probably being influenced by the orientation and steepness of the pre-inversion fault (Williams et al., 1989; Cooper et al., 1989; Cooper & Warren, 2010). Some structures of this type can still be followed for many kilometers having consistent geometry and attitude. These structures have not been much modified by reactivation and are invariably found in the proximal parts footwalls of master faults, suggesting that these are inversion structures that correlate to PSE-type 5-structures in the experiments developed in areas of focused contraction along pre-existing fault scarps during Miocene inversion.

Trains of folds with smaller amplitudes and higher frequency are sometimes found in fault blocks in the central part of the Vestbakken Volcanic Province (**Figure 12F**). Although these structures are not dateable by seismic stratigraphical methods (onlap configurations etc.) we regard these fold strains to be correlatable with the tight folds generated in the inversion stage in the experiments (PSE-6-structures) and that they are contemporaneous with the PSE-5-structures.

Segment 1 in the experiments, which corresponds to the Senja Shear Margin segment, displays a structural pattern that is a hybrid between segments 1 and 2. It contains incipient structural elements that were developed in full in segments 2 and 3, segment 2 being dominated by releasing and restraining bend configurations and segment 3 dominated by neutral shear. Due to internal configurations, the three segments were affected to secondary (oblique) opening and contraction in various fashions. Understanding these differences was much promoted by the comparison of seismic and model data.

Summary and conclusions

The Barents Shear Margin is a challenging target for structural analysis both because it represents a geometrically complex structural system with a multistage history, but also because high-quality (3D) seismic reflection data are limited and many structures and sedimentary systems generated in the earlier tectono-thermal stages have been overprinted and obliterated by younger events. This makes analogue experiments very useful in the analysis, since they offer a template for what kind of structural elements can be expected. By constraining the experimental model according to the outline of the margin geometry and imposing a dynamic stress model in harmony according to the state-of-the-art knowledge about the regional tectono-sedimentological development, we were able to interpret the observations done in seismic reflection data in a new light.

Our observations confirmed that the main segments of the Barents Shear Margin, albeit undergoing the same regional stress regime, display contrasting structural configurations. The deformation in segment 2 in the BarMar-experiments, was determined by releasing and restraining bends in the southern and northern parts, respectively. Thus, the southern part, corresponding to the Vestbakken Volcanic Province, was dominated by the development of a regional-scale extensional shear duplex. By continued shear the basin developed into a full-fledged pull-apart basin or rhomb graben in which rotating fault blocks were trapped. The pull-apart basin became the nucleus for greater basin systems to develop in the following phase of extension also providing the space for folds to develop in the contractional phase.

We conclude that fault- and fold systems found in the realm of the Vestbakken Volcanic Province are in accordance with a three-stage development that includes dextral shear followed by oblique extension and contraction (325/145^{0}) along a shear margin with composite geometry. Folds with NE-SW-trending fold axes are dominant in wider area of the Vestbakken Volcanic Province and are dominated by folds in the hanging walls of (older) normal faults, sometimes characterized by narrow, snakehead- or harpoon-type structures that are typical for tectonic inversion.

Comparing seismic mapping and analogue experiments it is evident that a main challenge in analyzing the structural pattern in shear margins of complex geometry and multiple reactivation is the low potential for preservation of structures that were generated in the earliest stages of the development.

Author contribution

R.H. Gabrielsen: Contributions to outline, design and performance of experiments. First writing and revisions of manuscript. First drafts of figures.

P.A. Giennenas: Seismic interpretation in the Vestbakken Volcanic Province. Identification and description of fold families.

D. Sokoutis: Main responsibility for set-up, performance and handling of experiments. Revisions of manuscript.

E. Willigshofer: Performance and handling of experiments. Revisions of manuscript. Design and revisions of figure material.

M. Hassaan: Background seismic interpretation. Discussions and revisions of manuscript. Design and revisions of figure material.

J.I. Faleide: Regional interpretations and design of experiments. Participation in performance and interpretations of experiments. Revisions of manuscript, design and revisions of figure material.

Acknowledgements

The work was supported by ARCEx (Research Centre for Arctic Petroleum Exploration), which was funded by the Research Council of Norway (grant number 228107) together with 10 academic and six industry (Equinor, Vår Energi, Aker BP, Lundin Energy Norway, OMV and Wintershall Dea) partners. Muhammad Hassaan was funded by the Suprabasins project (Research Council of Norway grant no. 295208). We thank to Schlumberger for providing us with academic licenses for Petrel software to do seismic interpretation. Two anonymous reviewers and the editors of this special volume provided comments, suggestions and advice that enhanced the clarity and sceienific quality of the paper.

References

Allemand, P. and Brun, J. P.: Width of continental rifts and rheological layering of the lithosphere. Tectonophysics, 188, 63-69, 1991.

Allmendinger, R. W.: Inverse and forward numerical modeling of threeshear fault-propagation folds, Tectonics, 17(4), 640-656, 1998.

Auzemery, A., Willingshofer, E., Sokoutis, D., Brun, J.- P., and Cloetingh, S. A. P. L.: Passive margin inversion controlled by stability of the mantle lithosphere, Tectonophysics, 817, 229042, 1-17, https://doi.org/10.1016/j.tecto.2021.229042, 2021.

Aydin, A. and Nur, A.: Evolution of pull-apart basins and their scale independence. Tectonics, 1, 91-105, 1982.

Ballard, J.-F., Brun, J.-P., and Van Ven Driessche, J.: Propagation des chevauchements au-dessus des zones de décollement: modèles expérimentaux. Comptes Rendus de l'Académie des Sciences, Paris, 11, 305, 1249-1253, 1987.

Basile, C.: Transform continental margins – Part 1: Concepts and models. Tectonophysics, 661, pp.1-10. doi: 10.1016/j.tecto.2015.08.034, 2015.

Basile, C. and Brun, J.-P.: Transtensional faulting patterns ranging from pull-apart basins to transform continental margins: an experimental investigation, Journal of Structural Geology, 21,23-37, 1997.

Beauchamp, W., Barazangi, M., Demnati, A., and El Alji, M.: Intracontinental rifting and inversion: Missour Basin and Atlas Mountains, Morocco. American Association of Petroleum Geologists Bulletin, 80(9), 1455-1482, 1996.

Bergh, S. G., Braathen, A., and Andresen, A.: Interaction of basement-involved and thin-skinned tectonism in the Tertiary fold-and-thrust belt of Central Spitsbergen, Svalbard. American Association of Petroleum Geologists Bulletin, 81(4), 637-661, 1997.

Bergh, S. G. and Grogan, P.: Tertiary structure of the Sørkapp-Hornsund Region, South Spitsbergen, and implications for the offshore southern extension of the fold-thrust-belt. Norwegian Journal of Geology, 83, 43-60, 2003.

Biddle, K. T. and Christie-Blick, N., (eds.): Strike-Slip Deformation, Basin Formation, and Sedimentation: Society of Economic Paleontologists and Mineralogists Special Publication, 37, 386 pp, 1985a.

Biddle, K. T. and Christie-Blick, N.: Glossary — Strike-slip deformation, basin formation, and sedimentation, in: Biddle, K. T. and Christie-Blick, N. (eds.): Strike-Slip Deformation, Basin Formation, and Sedimentation: Society of Economic Paleontologists and Mineralogists Special Publication, 37, 375-386, 1985b.

Blaich, O. A., Tsikalas, F., and Faleide, J. I.: New insights into the tectono-stratigraphic evolution of the southern Stappen High and the transition to Bjørnøya Basin, SW Barents Sea, Marine and Petroleum Geology, 85, 89-105, doi:

10.1016/j.marpetgeo.2017.04.015, 2017.

Breivik, A. J., Faleide, J. I., and Gudlaugsson, S. T.: Southwestern Barents Sea margin: late Mesozoic sedimentary basins and crustal extension, Tectonophysics, 293, 21-44, 1998.

Breivik, A. J., Mjelde, R., Grogan, P., Shinamura, H., Murai, Y., and Nishimura, Y.: Crustal structure and transform margin development south of Svalbard based on ocean bottom seismometer data. Tectonophysics, 369, 37-70, 2003.

Brekke, H.: The tectonic evolution of the Norwegian Sea continen- tal margin with emphasis on the Vøring and Møre basins: Geological Society, London, Special Publication, 136, 327–378, 2000.

Brekke, H. and Riis, F.: Mesozoic tectonics and basin evolution of the Norwegian Shelf between 60˚N and 72˚N. Norsk Geologisk Tidsskrift, 67, 295-322, 1987.

Burchfiel, B. C. and Stewart, J. H.: "Pull-apart" origin of the central segment of Death Valley, California. Geological Society of America Bulletin., 77, 439-442, 1966.

Campbell, J. D.: *En échelon* folding, Economical Geology, 53(4), 448-472, 1958.

Cartwright, J. A.: The kinematics of inversion in the Danish Central Graben. in: M.A.Cooper & G.D.Williams (eds.): Inversion Tectonics. Geological Society of London Special Publication, 44, 153-175, 1989.

Casas, A. M., Gapals, D., Nalpas, T., Besnard, K., and Román-Berdiel, T.: Analogue models of transpressive systems, Jornal of Structural Geology, 23,733-743, 2001.

Christie-Blick, N. and Biddle, K. T.: Deformation and basin formation along strike-slip faults. in: Biddle,K.T. & Christie-Blick,N. (eds.): Strike-slip deformation, basin formation and sedimentation. Society of Economic Mineralogists and Palaeontologists (Tulsa Oklahoma), Special Publication, 37, 1-34, 1985.

Cloos, H.: Experimenten zur inneren Tectonick, Zentralblatt für Mineralogie, Geologie und Palaentologie, 1928B, 609-621, 1928.

Cloos, H.: Experimental analysis of fracture patterns, Geological Society of America Bulletin, 66(3), 241-256, 1955.

Cooper, M. and Warren, M. J.: The geometric characteristics, genesis and petroleum significance of inversion structures, in Law,R.D., Butler,R.W.H., Holdsworth,R.E., Krabbendam,M. & Strachan,R.A. (eds.): Continental Tectonics and Mountain Building: The Lagacy of Peache and Horne, Geological Society of London, Special Publication, 335, 827-846, 2010.

Cooper, M. A., Williams, G. D., de Graciansky, P. C., Murphy, R. W., Needham, T., de Paor, D., Stoneley, R., Todd, S. P., Turner, J. P., and Ziegler, P. A.: Inversion tectonics – a discussion. Geological Society, London, Special Publications, 44, 335-347, 1989.

Coward, M.: Inversion tectonics, in: Hancock,P.L. (ed.): Continental Deformation, Pergamon Press, 289-304, 1994.

Coward, M. P., Gillcrist, R., and Trudgill, B.: Extensional structures and their tectonic inversion in the Western Alps, *in*: A.M.Roberts, G.Yielding & B.Freeman (eds.): The Geometry of Normal Faults. Geological Society of London Special Publication, 56, 93-112, 1991.

Crowell, J.: Displacement along the San Andreas Fault, California, Geological Society of America Special Papers, 71, 59pp, 1962.

Crowell, J. C.: Origin of late Cenozoic basins in southern California. in R.H.Dorr & R.H.Shaver (eds.): Modern and ancient geosynclinal sedimentation. SEPM Special Publication, 19, 292-303, 1974a.

Crowell, J. C.: Implications of crustal stretching and shortening of coastal Ventura Basin, in: Howell,D.G. (ed.): Aspects of the geological history of the Calefornia continental Borderland, American Association of Petroleum Geologists, Pacific Section, Publication 24, 365-382, 1974b.

Cunningham, W. D. and Mann,P. (eds.), 2007a: Tectonics of Strike-Slip Restraining and Releasing Bends, Geological Society London Special Publication, 290, 482pp.

Cunningham, W. D. and Mann, P.: Tectonics of Strike-Slip Restraining and Releasing Bends, *in:* Cunningham,W.D. & Mann,P. (eds.), 2007: Tectonics of Strike-Slip Restraining and Releasing Bends, Geological Society London Special Publication, 290, 1-12, 2007b.

Dauteuil, O. and Mart, Y.: Analogue modeling of faulting pattern, ductile deformation, and vertical motion in strike-slip fault zones, Tectonics, 17(2), 303-310, 1998.

Del Ventisette, C., Montanari, D., Sani, F., Bonini, M., and Corti, G.: Reply to comment by J. Wickham on ‘‘Basin inversion and fault reactivation in laboratory experiments’’. Journal of Structural Geology 29, 1417–1418, 2007.

Dooley, T. and McClay, K.: Analog modeling of pull-apart basins, American Association of Petroleum Geologists Bulletin, 81(11), 1804-1826, 1997.

Dooley, T. P. and Schreurs, G.: Analogue modelling of intraplate strike-slip tectonics: A review and new experimental results, Tectonophysics, 574-575, 1-71, 2012.

Doré, A. G. and Lundin, E. R.: Cenozoic compressional structures on the NE Atlantic margin: nature, origin and potential significance for hydrocarbon exploration. Petroleum Geosciences, 2, 299-311, 1996.

Doré, A. G., Lundin, E. R., Gibbons, A., Sømme, T. O., and Tørudbakken, B. O.: Transform margins of the Arctic: a synthesis and re-evaluation *in:* Nemcok,M., Rybár,S., Sinha,S.T., Hermeston,S.A. & Ledvényiová,L. (eds.): Transform Margins,:

Development, Control and Petroleum Systems, Geological Society London, Special Publication, 431, 63-94, 2016.

Doré, A. G., Lundin, E. R., Jensen, L. N., Birkeland, Ø., Eliassen, P. E., and Fichler, C.: Principal tectonic events in the evolution of the northwest European Atlantic margin. In: A.J.Fleet & S.A.R.Boldy (eds.): Petroleum Geology of Northwest Europe: Proceedings of the Fifth Conference (Geological Society of London), 41-61, 1999.

Eidvin, T., Goll, R. M., Grogan, P., Smelror, M., and Ulleberg, K.: The Pleistocene to Middle Eocene stratigraphy and geological evolution of the western Barents Sea continental margin ta well site 731675-1 (Bjørnøya West area). Norsk Geologisk Tidsskrift, 78, 99-123, 1998.

Eidvin, T., Jansen, E., and Riis, F.: Chronology of Tertiary fan deposits off the western Barents Sea: Implications for the uplift and erosion history of the Barents Shelf. Marine Geology, 112, 109-131, 1993.

Eldholm,O., Faleide,J.I. & Myhre,A.M., 1987: Continent-ocean transition at the western Barents Sea/Svalbard continental margin. Geology, 15, 1118-1122.

Eldholm, O., Thiede, J., and Taylor, E.: Evolution of the Vøring volcanic margin, *in:* Eldholm, O., Thiede, J., and Taylor, E., (eds.): Proceedings of the Ocean Drilling Program, Scientific Results, 104: College Station (Ocean Drilling Program), TX, 1033–1065, 1989.

Eldholm, O., Tsikalas, F., and Faleide, J. I.: Continental margin off Norway 62-75^{o}N:Paleogene tectono-magmatic segmentation and sedimentation. Geological Society of London Special Publication, 197, 39-68, 2002.

Emmons, R. C.: Strike-slip rupture patterns in sand models, Tectonophysics, 7, 71-87, 1969.

Faugère, E., Brun, J.-P., and Van Den Driessche, J.: Bassins asymmétriques en extension pure et en détachements:Modèles expérimentaux, Bulletin Centre Recherche Exploration et Production Elf Aquitaine, 10(2), 13-21, 1986.

Faleide, J. I., Bjørlykke, K., and Gabrielsen, R. H.: Geology of the Norwegian Shelf. *in*: Bjørlykke,K.: Petroleum Geoscience: From Sedimentary Environments to Rock Physics 2^{nd} Edition, Springer-Verlag, Berlin Heidelberg, Chapter 25, 603 -637, 2015.

Faleide, J. I., Myhre, A. M., and Eldholm, O.: Early Tertiary volcanism at the western Barents Sea margin. in: A.C.Morton & L.M.Parsons (eds.): Early Tertiary volcanism and the opening of the NE Atlantic.Geological Society of London Special Publication, 39,135-146, 1988.

Faleide, J. I., Tsikalas, F., Breivik, A. J, Mjelde, R., Ritzmann, O., Engen, Ø., Wilson, J., and Eldholm, O.: Structure and evolution of the continental margin off Norway and the Barents Sea. Episodes, 31(1), 82-91, 2008.

Faleide, J. I., Vågnes, E., and Gudlaugsson, S. T.: Late Mesozoic - Cenozoic evolution of the south-western Barents Sea in a regional rift-shear tectonic setting. Marine and Petroleum Geology, 10, 186-214, 1993.

Fichler, C. and Pastore, Z.: Petrology and crystalline crust in the southwestern Barents Sea inferred from geophysical data. Norwegian Journal of Geology, 102, 41pp, https://dx.doi.org/10.17850/njg102-2-2, 2022.

Freund, R.: The Hope Fault, a strike-slip fault in New Zealand, New Zealand Geological Survey Bulletin, 86, 1-49, 1971.

Gabrielsen, R. H.: Structural elements in graben systems and their influence on hydrocarbon trap types. in: A.M. Spencer (ed.): Habitat of Hydrocarbons on the Norwegian Continental Shelf. Norw. Petrol. Soc. (Graham & Trotman), 55 – 60, 1986.

Gabrielsen, R. H., Færseth, R. B., Jensen, L. N., Kalheim, J. E., and Riis, F.: Structural elements of the Norwegian Continental Shelf. Part I: The Barents Sea Region. Norwegian Petroleum Directorate, Bulletin, 6, 33pp, 1990.

Gabrielsen, R. H., Grunnaleite, I., and Rasmussen, E.: Cretaceous and Tertiary inversion in the Bjørnøyrenna Fault Complex, south-western Barents Sea. Marine and Petroleum Geology, 142, 165-178, 1997.

Gac, S., Klitzke, P., Minakov, A., Faleide, J. I., and Scheck-Wenderoth, M.: Lithospheric strength and eleastic thickness of the Barents Sea and Kara Sea region, Tectonophysics, 691, 120-132, doi: 10.106/j.tecto.2016.04.028, 2016.

Gaina, C., Gernigon, L., and Ball, P.: Palaeocene – Recent plate boundaries in the NE Atlantic and the formation of the Jan Mayen microcontinent. Journal of the Geological Society, London, 166(4), 601-616, 2009.

Ganerød, M., Smethurst, M. A., Torsvik, T. H., Prestvik, T., Rousse, S., McKenna, C., van Hinsberen, D.J.J., and Hendriks, W. W. H.: The North Atlantic Igneous Province reconstructed and its relation to the Plume Generation Zone: the Antrim Lava Group revisited. Geophysical Journal International, 182, 183-202, doi: 10.1111/j.1365-246X.2010.04620.x, 2010.

Giennenas, P. A.: The Strucural Development of the Vestbakken Volcanic Province, Western Barents Sea. Relation between Faults and Folds, Unpubl. Master thesis, University of Oslo, 89 pp, 2018.

Graymer, R. W., Langenheim, V. E., Simpson, R. W., Jachens, R. C., and Ponce, D. A.: Relative simple through-going fault planes at large-earthquake depth may be concealed by surface complexity of strike-slip faults, *in*: Cunningham,W.D. & Mann,P. (eds.): Tectonics of Strike-Slip Restraining and Releasing Bends, Geological Society London Special Publication, 290, 189-201, 2007.

Griera, A., Gomez Rivas, E., and Llorens, M.- G.: The influence of layer-interface geometry of single-layer folding. Geological Society of London Special Publication 487, SP487:4, 2018.

Grogan, P., Østvedt-Ghazi, A.- M., Larssen, G. B., Fotland, B., Nyberg, K., Dahlgren, S., and Eidvin, T.: Structural elements and petroleum geology of the Norwegian sector of the northern Barents sea. *in*: Fleet,A.J. & Boldry,S.A.R. (eds.): Petroleum Geology of Northwest Europe: Proceedings of the 5th Conference, Geological Society of London, 247-259, 1999.

Groshong, R. H.: Half-graben structures: balanced models of extensional fault bend folds, Geological Society of America Bulletin, 101, 96-195, 1989.

Gudlaugsson, S. T. and Faleide, J. I.: The continental margin between Spitsbergen & Bjørnøya, in: O.Eiken (ed.): Seismic Atlas of Western Svalbard, Norsk Polarinstitutt Meddelelser, 130, 11-13, 1994.

Gudlaugsson, S. T., Faleide, J. I., Johansen, S. E., and Breivik, A. J.: Late Palaeozoic structural development of the south-western Barents Sea. Marine and Petroleum Geology, 15, 73-102, 1998.

Hamblin, W. K.: Origin of "reverse drag" on the down-thrown side of normal faults, Geological Society of America Bulletin, 76, 1145-1164, 1965.

Hanisch, J.: The Cretaceous opening of the Northeast Atlantic. Tectonophysics, 101, 1-23, 1984.

Harding, T. P.: Petroleum traps associated with wrench faults. American Association of Petroleum Geologists Bulletin, 58, 1290-1304, 1974.

Harding, T. P. and Lowell, J. D.: Structural styles, their plate tectonic habitats, and hydrocarbon traps in petroleum provinces, American Association of Petroleum Geologists Bulletin, 63,1016-1058, 1979.

Harland, W. B.: The tectonic evolution of the Arctic-North Atlantic Region, in: Taylor,J.H., Rutten,M.G., Hales,A.L., Shackelton,R.M., Nairn,A.E. & Harland:W.B.,: Discussion, A Symposium on Continental Drift, Philosophical Transactions of the Royal Society of London,, Series A, 258, 1088, 59-75, 1965.

Harland, W. B.: Contributions of Spitsbergen to understanding of tectonic evolution of North Atlantic Region, American Association of Petroleum Geologists, Memoir 12, 817-851, 1969.

Harland, W. B.: Tectonic transpression in Caledonian Spitsbergen, Geological Magazine, 108, 27-42, 1971.

Henk, A. and Nemcok, M.: Stress and fracture prediction in inverted half-graben structures. Journal of Structural Geology, 30(1), 81-97, 2008.

Horni, J. Á., Hopper, J. R., Blischke, A., Geisler, W. H., Stewart, M., Mcdermott, K., Judge, M., Erlendsson, Ö, and Árting, U. E.: Regional Distribution of Volcanism within the North Atlantic Igneous Province. The NE Atlantic Region: A Reappraisal of Crustal Structure, Tectonostratigraphy and Magmatic Evolution. Geological

Society, London, Special Publications, 447, 105–125, https://doi.org/10.1144/SP447.18, 2017.

Horsfield, W. T.: An experimental approach to basement-controlled faulting. Geologie en Mijbouw, 56(4), 3634-370, 1977.

Hubbert, M. K.: Theory of scale models as applied to the study of geologic structures, Bulletin Geological Society of America, 48, 1459-1520, 1937.

Jebsen, C. and Faleide, J. I.: Tertiary rifting and magmatism at the western Barents Sea margin (Vestbakken volcanic province). III international conference on Arctic margins, ICAM III; abstracts; plenary lectures, talks and posters, 92, 1998.

Khalil, S. M. and McClay, K. R.: 3D geometry and kinematic evolution of extensional fault-related folds, NW Red Sea, Egypt. in: Childs,C., Holdswort,R.E., Jackson,C.A.L., Manzocchi,T., Walsh,J.J & Yielding,G. (eds.): The Geometry and Growth of Normal Faults, Geological Society, London, Special Publication 439, doi.org/10.1144/SP439.11, 2016.

Klinkmüller, M., Schreurs, G., Rosenau, M., and Kemnitz, H.: Properties of granular analogue model materials: a community wide survey. Tectonophysics 684, 23–38. http://dx.doi.org/10.1016/j.tecto.2016.01.017.feb., 2016.

Knutsen, S.-M. and Larsen, K. I.: The late Mesozoic and Cenozoic evolution of the Sørvestsnaget Basin: A tectonostratigraphic mirror for regional events along the Southwestern Barents Sea Margin? Marine and Petroleum Geology, 14(1), 27-54, 1997.

Kristensen, T. B., Rotevatn, A., Marvik, M., Henstra, G. A., Gawthorpe, R. L. and Ravnås, R.: Structural evolution of sheared basin margins: the role of strain partitioning. Sørvestsnaget Basin, Norwegian Barents Sea, Basin Research, 2017), 1-23, doi:10.1111/bre.12235, 2017.

Le Calvez, J.-H. and Vendeville, B. C.: Experimental designs to mode along strike-slip fault interaction. *in*: Scellart,W.P. & Passcheir,C. (eds.). Analogue Modeling of large-scale Tectonic Processes, Journal of Virtual Explorer, 7, 7-23, 2002.

Leever, K. A., Gabrielsen, R. H., Sokoutis, D. and Willingshofer, E.: The effect of convergence angle on the kinematic evolution of strain partitioning in transpressional brittle wedges: insight from analog modeling and high resolution digital image analysis. Tectonics, 30, TC2013, 1-25, doi: 10.1029/2009TC002649, 2011a.

Leever, K. A., Gabrielsen, R. H., Faleide, J. I. and Braathen, A.: A transpressional origin for the West Spitsbergen Fold and Thrust Belt - insight from analog modeling. Tectonics, 30, TC2014, 1- 24, doi: 10.1029/2010TC002753, 2011b.

Libak, A., Mjelde, R., Keers, H., Faleide, J. I. and Murai, Y.: An intergrated geophysical study of Vestbakken Volcanic Province, western Barents Sea continental margin, and adjacent oceanic crust, Marine Geophysical Research, 33(2), 187-207, 2012a.

Libak, A., Eide, C. H., Mjelde, R., Keers, H., and Flüh, E. R.: From pull-apart basins to ultraslow spreading: Results from the western Barents Sea Margin. Tectonophysics, 514–517, 44–61, 2012b.

Lorenzo, J. M.: Sheared continental margins: an overview, Geo-Marine Letters, 17(1), 1-3, 1997.

Lowell, J. D.: Spitsbergen Tertiary orogenic belt and the Spitsbergen fracture zone, Geol. Soc. Am. Bull., 83, 3091–3102, doi:10.1130/0016-7606(1972)83[3091:STOBAT]2.0.CO;2, 1972.

Lundin, E. R. and Doré, A. G.: A tectonic model for the Norwegian passive margin with implications for the NE Atlantic.: Early Cretaceous to break-up. Journal of the Geological Society London, 154, 545-550, 1997.

Lundin, E. R., Doré, A. G., Rønning, K. and Kyrkjebø, R.: Repeated inversion in the Late Cretaceous-Cenozoic northern Vøring Basin, offshore Norway, Petroleum Geoscience, 19(4), 329-341, 2013.

Luth, S., Willingshofer, E., Sokoutis, D. and Cloetingh, S.: Analogue modelling of continental collision: Influence of plate coupling on manle lithosphere subduction, crustal deformation and surface topography, Tectonophysics, 4184, 87-102, doi: 10.1016/j.tecto2009.08.043, 2010.

Maher, H. D., Jr., Bergh, S., Braathen, A., and Ohta, Y.: Svartfjella, Eidembukta, and Daudmannsodden lineament: Tertiary orogen-parallel motion in the crystalline hinterland of Spitsbergen's fold-thrust belt, Tectonics, 16(1), 88–106, doi:10.1029/96TC02616, 1997.

Mandl, G., de Jong, L. N. J., and Maltha, A.: Shear zones in granular material. Rock Mechanics, 9, 95–144, 1977.

Manduit, T. and Dauteuil, O.: Small scale modeling of oceanic transform zones, Journal of Geophysical Research, 101(B9), 20195-20209, 1996.

Mann, P.: Global catalogue, classification and tectonic origins o frestraining and releasing bends on active and ancient strike-slip fault systems. *in*: Cunningham,W.D. & Mann,P. (eds.), 2007: Tectonics of Strike-Slip Restraining and Releasing Bends, Geological Society London Special Publication, 290, 13-142, 2007.

Mann, P., Hempton, M. R., Bradley, D. C., and Burke, K.: Development of pull-apart basins. Journal of Geology, 91(5), 529-554, 1983.

Mascle, J. and Blarez, E.: Evidence for transform margin evolution from the Ivory Coast Ghana continental margin, Nature, 326, 378-381, 1987.

McClay, K. R.: Extensional fault systems in sedimentary basins. A review of analogue model studies, Marine and Petroleum Geology, 7, 206-233, 1990.

Mitra, S.: Geometry and kinematic evolution of inversion structures. American Assiciation of Petroleum Geologists Bulletin, 77, 1159-1191, 1993.

Mitra, S. and Paul, D.: Structural geology and evolution of releasing and constratrining bends: Insights from laser-scanned experimental models, American Association of Petroleum Geologists Bulletin, 95(7), 1147-1180, 2011.

Morgenstern, N. R. and Tchalenko, J. S.: Microscopic structures in kaolin subjected to direct shear, Géotechnique, 17, 309-328, 1967.

Mosar, J., Torsvik, T. H., and the BAT Team: Opening of the Norwegian and Greenland Seas: Plate tectonics in mid Norway since the late Permian. in: E.Eide (ed.): BATLAS. Mid Norwegian plate reconstruction atlas with global and Atlantic perspectives. Geological Survey of Norway, 48-59, 2002.

Mouslopoulou, V., Nicol, A., Little, T. A., and Walsh, J. J.: Terminations of large-strike-slip faults: an alternative model from New Zealand, in: Cunningham,W.D. & Mann,P. (eds.): Tectonics of Strike-Slip Restraining and Releasing Bends, Geological Society London Special Publication, 290, 387- 415, 2007.

Mouslopoulou, V., Nicol, A., Walsh, J. J., Beetham, D., and Stagpoole, V.: Quaternary temporal stability of a regional strike-slip and rift fault interaction. Journal of Structural Geology, 30, 451-463, 2008.

Myhre, A. M. and Eldholm, O.: The western Svalbard margin (74-80°N). Marine and Petroleum Geology, 5, 134-156, 1988.

Myhre, A. M., Eldholm, O., and Sundvor, E.: The margin between Senja and Spitsbergen Fracture Zones: Implications from plate tectonics. Tectonophysics, 89, 33-50, 1982.

Naylor, M. A., Mandl, G., and Sijpestijn, C. H. K.: Fault geometries in basement-induced wrench faulting under different initial stress states. Journal of Structural Geology, 8, 737-752, 1986.

Nemcok, M., Rybár, S., Sinha, S. T., Hermeston, S. A., and Ledvényioviá, L.: Transform margins: development, controls and petroeum systems – an introduction. in: Nemcok,M., Rybár,S., Sinha,S.T., Hermeston,S.A. & Ledvényiová,L. (eds.): Transform Margins,: Development, Control and Petroleum Systems, Geological Society London, Special Publication, 431, 1-38, 2016.

Odonne, F. and Vialon, P.: Analogue models of folds above a wrench fault, Tectonophysics, 990,31-46, 1983.

Pace, P. and Calamita, F.: Push-up inversion structures v. fault-bend reactivation anticlines along oblique thrust ramps: examples from the Apennines fold-and-thrust-belt, Italy, Journal Geological Society London, 171, 227-238, 2014.

Pascal, C. and Gabrielsen, R. H.: Numerical modelling of Cenozoic stress patterns in the mid Norwegian Margin and the northern North Sea. Tectonics, 20(4), 585-599, 2001.

Pascal, C., Roberts, D., and Gabrielsen, R. H.: Quantification of neotectonic stress orientations and magnitudes from field observations in Finnmark, northern Norway. Journal of Structural Geology, 27, 859-870, 2005.

Peacock, D. C. P., Nixon, C. W., Rotevatn, A., Sanderson, D. J., and Zuluaga, L. F.: Glossary of fault and other fracture networks, Journal of Structural Geology, 92, 12-29, doi: 10.1016/j.jgs2016.09.008, 2016.

Perez-Garcia, C., Safranova, P. A., Mienert, J., Berndt, C., and Andreassen, K.: Extensional rise and fall of a salt diapir in the Sørvestsnaget Basin, SW Barents Sea. Marine and Petroleum Geology, 46, 129-134, 2013.

Planke, S., Alvestad, E., and Eldholm, O.: Seismic characteristics of basaltic extrusive and intrusive rocks: The Leading Edge, 18(3), 342-348. https://doi-org.ezproxy.uio.no/10.1190/1.1438289, 1999.

Ramberg, H.: Gravity, deformation and the Earth's crust, Academic Press, New York, 214pp, 1967.

Ramberg, H.: Gravity, deformation and the Earth's crust, 2nd edition. Academic Press, New York 452pp, 1981.

Ramsay, J. G. and Huber, M. I.: The techniques of modern structural geology. Vol. 2: Folds and fractures. Academic Press, London, 309-700, 1987.

Reemst, P., Cloetingh, S., and Fanavoll, S.: Tectonostratigraphic modelling of Cenozoic uplift and erosion in the south-western Barents Sea. Marine and Petroleum Geology, 11, 478-490, 1994.

Richard, P. D., Ballard, B., Colletta, B., and Cobbold, P. R.: Naissance et evolution de failles au dessus d'un décrochement de socle: Modeléisation experimental et tomographie, C. R. Acad.Sci. Paris, 308,9, 2111-2118, 1989.

Richard, P. D. and Cobbold, P. R.: Structures et fleur positives et décrochements crustaux: mdélisation analogiuque et interpretation mechanique, C.R.Acad.Sci.Paris, 308, 553-560, 1989.

Richard, P. and Krantz, R. W.: Experiments on fault reactivation in strike-slip mode, Tectonophysics, 188, 117-131, 1991.

Richard, P., Mocquet, B., and Cobbold, P. R.: Experiments on simultaneous faulting and folding above a basement wrench fault, Tectonophysics, 188, 133-141, 1991.

Riedel, W.: Zur Mechanik geologischer Brucherscheinungen. Centralblatt für Mineralogie, Geologie und Palentologie, 1929B, 354-368, 1929.

Riis, F., Vollset, J., and Sand, M.: Tectonic development of the western margin of the Barents Sea and adjacent areas. in: M.T.Halbouty (ed.): Future petroleum provinces of the World. American Association of Petroleum Geologists Memoir, 40, 661-667, 1986.

Roberts, D. G.: Basin inversion in and around the British Isles, in: M.A.Cooper & G.D.Williams (eds.): Inversion Tectonics. Geological Society of London Special Publication, 44, 131-150, 1989.

Ryseth, A., Augustson, J. H., Charnock, M., Haugsrud, O., Knutsen, S.-M., Midbøe, P. S., Opsal, J. G. and Sundsbø, G.: Cenozoic stratigraphy and evolution of the Sørvestsnaget Basin, southwestern Barents Sea. Norwegian Journal of Geology, 83, 107-130, 2003.

Saunders, A. D., Fitton, J. G., Kerr, A. C., Norry, M. J., and Kent, R. W.: The North Atlantic Igneous Province: Geophysical Monograph 100, American Geophysical Union, pp. 45–93, 1997.

Scheurs, G.: Experiments on strike-slip faulting and block rotation, Geology, 22,567-570, 1990.

Schreurs, G.: Fault development and interaction in distributed strike-slip shear zones: an experimental approach. *in:* Storti,F., Holdsworth,R.E. & Salvini,F. (eds): Intraplate Strike-slip Deformation Belts, Geological Society of London Special Publication, 210, 35-82, 2003.

Schreurs, G., Colletta, B.: Analogue modelling of faulting in zones of continental transpression and transtension. *in:* Holdsworth, R.E., Strachan, R.A., Dewey, J.F. (eds.), Continental Transpressional and Transtensional Tectonics, Geological Society of London Special Publication, London, 135, 59–79, 1998.

Schreurs, G. and Colletta, B.: Analogue modelling of continental transpression and transtension. *in:* Scellart,W.P. & Passchier,C. (eds.): Analogue Modelling of Large-scale Tectonic Processes. Journal of the Virtual Explorer, 7, 103-114, 2003.

Seiler, C., Fletcher, J. M., Quigley, M. C., Gleadow, A. J. and Kohn, B. P.: Neogene structural evolution of the Sierra San Felipe, Baja California: evidence of proto-gulf transtension in the Gulf Extensional Province? Tectonophysics, 488(1), 87-109, 2010.

Sims, D., Ferrill, D. A., and Stamatakos, J. A.: Role of a brittle décollement in the development of pull-apart basins : experimental results and natural examples. Journal of Structural Geology, 21, 533-554, 1999.

Sokoutis, D.: Finite strain effects in experimental mullions. Journal of Structural Geology, 9, 233-249, 1987.

Stearns, D. W.: Faulting and forced folding in the Rocky Mountains Foreland, Geological Society of America Memoir, 151, 1-38, 1978.

Sylvester, A. G. (ed): Wrench Fault Tectonics, Selected papers reprinted from the AAPG Bulletin and other geological journals, American Association of Petroleum Geologists Reprint Series 28,3 74pp, 1985.

Sylvester, A. G.: Strike-slip faults. Geological Society of America Bulletin, 100, 1666-1703, 1988.

Talwani, M. and Eldholm, O.: Evolution of the Norwegian-Greenland Sea. Geological Society of America Bulletin, 88, 969-999, 1977.

Tchalenko, J. S.: Similarities between shear zones of different magnitudes. Geological Society of America Bulletin, 81, 1625-1640, 1970.

Tron, V. and Brun, J.-P.: Experiments on oblique rifting in brittle-ductile systems. Tectonophysics, 188(1/2), 71-84, 1991.

Tsikalas, F., Faleide, J. I., Eldholm, O., and Blaich, O. A.: The NE Atlantic conjugate Margins. In: Roberts, D.G. & Bally, A.W., Phanerozoic Passive Margins, Cratonic Basins and Global Tectonic Maps, Elsevier, DOI: 10.1016/B978-0-444-56357-6.00004-4, 2012.

Twiss, R. J. and Moores, E. M.: Structural Geology, 2nd Edition, W.H.Freeman & Co., New York, 736pp, 2007.

Ueta, K., Tani, K. and Kato, T.: Computerized X-ray tomography analysis of three-dimensional fault geometries in basement-induced wrench faulting, Engineering Geology, 56, 197-210, 2000.

Uliana, M. A., Arteaga, M. E., Legarreta, L., Cerdan, J.J. and Peroni, G. O.: Inversion structures and hydrocarbon occurrence in Argentia. *in*: Buchanan,J.G. & Buchanan,P.G. (eds.): Basin Inversion, Geological Society London Special Publication, 88, 211-233, 1995.

Vågnes, E.: Uplift at thermo-mechanically coupled ocean-continent transforms: modeled at the Senja Fracture Zone, southwestern Barents Sea. Geo-Marine Letters, 17, 100-109, 1997.

Vågnes, E., Gabrielsen, R. H., and Haremo, P.: Late Cretaceous-Cenozoic intraplate contractional deformation at the Norwegian continental shelf: timing, magnitude and regional implications. Tectonophysics, 300, 29-46, 1998.

Weijermars, R. and Schmeling, H.: Scaling of Newtonian and non-Newtonian fluid dynamics without inertia for quantitative modelling of rock flow due to gravity (including the concept of rheological similarity. Physics of the Earth and Planetary Interiors, 43, 316–330, 1986.

Wilcox, R. E., Harding, T. P., and Selly, D. R.: Basic wrench tectonics. American Association of Petroleum Geologists Bulletin, 57, 74-69, 1973.

Williams, G. D., Powell, C. M., and Cooper, M. A.: Geometry and kinematics of inversion tectonics. in: M.A.Cooper & G.D.Williams (eds.): Inversion Tectonics. Geological Society of London Special Publication, 44, 3-16, 1989.

Willingshofer, E., Sokoutis, D., and Burg, J.- P.: Lithosprer-scale analogue modelling of collsion zones with a pre-existing weak zone, *in*: Gapais,D., Brun.,J.P.& Cobbold,P.R. (eds.): DeformatiomMechanisms, Rhology and Tectonics: from Minerals to the Litohsphere, Geological Society London Special Publication,43, 277-294, 2005.

Willingshofer, E., Sokoutis, D., Beekman, Schönebeck, F., Warsitzka, J.-M., Michael, M., and Rosenau, M.: Ring shear test data of feldspar sand and quartz sand used in the Tectonic Laboratory (TecLab) at Utrecht University for experimental Earth Science applications. V. 1. GFZ Data Service. https://doi.org/10.5880/fidgeo.2018.072, 2018.

Woodcock, N. H. and Fisher, M.: Strike-slip duplexes. Journal of Structural Geology, 8(7), 725-735, 1986.

Woodcock, N. H. and Schubert, C.: Continental strike-slip tectonics. in: P.L.Hancock (ed.): Continental Deformation (Pergamon Press), 251-263, 1994.

Yamada, Y. and McClay, K. R.: Analog modeling of inversion thrust structures, experiments of 3D inversion structures above listric fault systems, in: McClay,K.R. (ed.): Thrust Tectonics and Petroleum Systems, American Association of Petroleum Geologists Memoir, 82, 276-302, 2004.